ACS ENVIRONMENTAL Au
AN OPEN ACCESS JOURNAL OF THE AMERICAN CHEMICAL SOCIETY

Editors' Choice
Open Access

pubs.acs.org/environau

Article

Long-Term Robustness and Failure Mechanisms of Electrochemical Stripping for Wastewater Ammonia Recovery

Published as part of ACS Environmental Au virtual special issue "2023 Rising Stars in Environmental Research".

Anna Kogler, Neha Sharma, Diana Tiburcio, Meili Gong, Dean M. Miller, Kindle S. Williams, Xi Chen, and William A. Tarpeh*

Cite This: *ACS Environ. Au* 2024, 4, 89–105

Read Online

ACCESS | Metrics & More | Article Recommendations | Supporting Information

ABSTRACT: Nitrogen in wastewater has negative environmental, human health, and economic impacts but can be recovered to reduce the costs and environmental impacts of wastewater treatment and chemical production. To recover ammonia/ammonium (total ammonia nitrogen, TAN) from urine, we operated electrochemical stripping (ECS) for over a month, achieving 83.4 ± 1.5% TAN removal and 73.0 ± 2.9% TAN recovery. With two reactors, we recovered sixteen 500-mL batches (8 L total) of ammonium sulfate (20.9 g/L TAN) approaching commercial fertilizer concentrations (28.4 g/L TAN) and often having >95% purity. While evaluating the operation and maintenance needs, we identified pH, full-cell voltage, product volume, and water flux into the product as informative process monitoring parameters that can be inexpensively and rapidly measured. Characterization of fouled cation exchange and omniphobic membranes informs cleaning and reactor modifications to reduce fouling with organics and calcium/magnesium salts. To evaluate the impact of urine collection and storage on ECS, we conducted experiments with urine at different levels of dilution with flush water, extents of divalent cation precipitation, and degrees of hydrolysis. ECS effectively treated urine under all conditions, but minimizing flush water and ensuring storage until complete hydrolysis would enable energy-efficient TAN recovery. Our experimental results and cost analysis motivate a multifaceted approach to improving ECS's technical and economic viability by extending component lifetimes, decreasing component costs, and reducing energy consumption through material, reactor, and process engineering. In summary, we demonstrated urine treatment as a foothold for electrochemical nutrient recovery from wastewater while supporting the applicability of ECS to seven other wastewaters with widely varying characteristics. Our findings will facilitate the scale-up and deployment of electrochemical nutrient recovery technologies, enabling a circular nitrogen economy that fosters sanitation provision, efficient chemical production, and water resource protection.

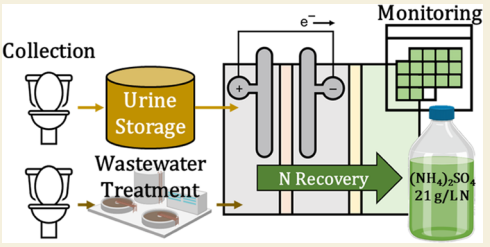

KEYWORDS: *circular economy, electrolysis, nitrogen, operation and maintenance, resource recovery, urine*

1. INTRODUCTION

Nitrogen in wastewater has negative environmental, human health, and economic impacts.[1−3] However, nitrogen as ammonia, which occurs in high concentrations in streams such as hydrolyzed (i.e., ureolyzed or after urea hydrolysis) urine,[4,5] can be harnessed as a valuable resource.[6] In fact, nitrogen excreted via urine could replace about 15% of nitrogen fertilizers worldwide.[7,8] Incumbent municipal wastewater nitrogen removal requires substantial chemical and energy inputs, with wastewater treatment accounting for about 2% of electrical energy consumption in the United States.[9,10] Meanwhile, ammonia synthesis via the Haber-Bosch process accounts for about 1% of global fossil fuel energy consumption[11] and 1.4% of global carbon dioxide emissions.[12] Recovering nitrogen from wastewater, particularly from highly concentrated streams like urine, for beneficial reuse in a circular economy can reduce the environmental impacts and costs of wastewater treatment and chemical production.

Electrochemical processes comprise an emerging type of wastewater treatment technology that is well-suited for nutrient (e.g., nitrogen) recovery but requires further study.[13,14] Electrochemical processes can easily be scaled to treat varying flow rates and facilitate *in situ* production of chemicals, enabling decentralized treatment.[15−18] While facilitating targeted total ammonia nitrogen [TAN; the sum of ammonia (NH_3) and ammonium (NH_4^+)] recovery, some electrochemical treatment processes can simultaneously achieve other benefits, such as pharmaceutical removal, electricity generation, and pathogen disinfection.[13,15] Many

Received: September 21, 2023
Revised: December 14, 2023
Accepted: December 22, 2023
Published: January 12, 2024

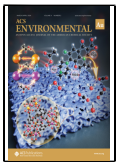

electrochemical ammonia recovery technologies, including electrodialysis,[19,20] capacitive deionization,[21,22] and electrochemical stripping (ECS),[23] have been demonstrated at lab scale. Batch and continuous ECS treatment of urine has been demonstrated,[23] along with batch treatment of effluent from wastewater algae hydrothermal liquefaction[24] and anaerobic digestate from fecal sludge.[25] ECS application across a range of influent ammonium concentrations (30 to 3,000 mg/L TAN) also appears feasible based on experiments and an accompanying process performance model.[25] When treating urine, ECS recovers an ammonium sulfate product with negligible pharmaceutical contamination based on target analysis of 11 compounds.[23] These promising advances in electrochemical nutrient recovery motivate further investigation to accelerate technologies toward real-world application.

Several process engineering gaps must be addressed to facilitate scale-up and widespread implementation of electrochemical nutrient treatment technologies, including ECS. Common barriers include integration into treatment trains; product characteristics and acceptable applications; optimization of operating conditions, reactor configuration, and materials; and gaps between experimental data and modeling efforts related to life cycle and cost evaluation.[15,26] Moreover, long-term studies evaluating robustness in realistic operating environments are limited for electrochemical nutrient technologies compared to other nutrient technologies and electrochemical technologies. In terms of electrochemical nutrient technologies, electrochemical magnesium dosing for struvite ($NH_4MgPO_4{\cdot}6H_2O$) recovery from urine has been applied to urine for 4 days,[27] a hydrogen-recycling electrochemical system coupled with membrane stripping has been tested for TAN recovery from urine for 7 days,[28] and electrodialysis has been demonstrated for anaerobic digestate from solids processing at a wastewater treatment plant for 3 days.[29] In comparison, other nutrient technologies, such as nitrification−distillation, have been operated for several months to 3.5 years in studies and longer in practice.[30−32] Electrochemical technologies with non-nutrient targets (e.g., electrochemical oxidation of wastewater) have also been demonstrated for about one month.[33] To date, ECS has been evaluated for up to 24 h with constant influent composition,[23] demonstrating the need for evaluation during longer operation.

Long-term investigations address barriers facing electrochemical nutrient recovery technologies by providing insights into reactor component degradation, failure mechanisms (e.g., ion exchange membrane fouling,[34] electrode inactivation[35−38]), and performance changes with longer operation. Such studies elucidate the impact of influent composition on performance, as well as pre- and post-treatment processes and maintenance tasks needed to sustain consistent operation and effluent quality despite varying influents. Long-term operation also requires measurable indicator metrics that help diagnose maintenance needs.[39] Some considerations of long-term operation are shared among both nutrient-focused electrochemical technologies and other electrochemical techniques, such as electrolysis (e.g., in the chlor-alkali industry[40]), electrodialysis (e.g., for potable water production from brackish water[41]), and electrodeionization (e.g., at nuclear power plants[42]). However, some aspects are unique to nutrient recovery and applications to excreta-derived waste streams. Thus, a long-term study of ECS could inform the development and implementation of other electrochemical nutrient treatment processes due to the similarity of operating mechanisms and reactor construction across many technologies.

This study demonstrates and investigates electrochemical nutrient recovery in diverse wastewaters under long-term operation. Specifically, we (1) evaluated nutrient removal and recovery performance when treating multiple wastewaters; (2) investigated performance stability, failure mechanisms, and monitoring methods during long-term operation; and (3) demonstrated the robustness of ECS performance when exposed to influent urine variability. The demonstrated operation of ECS for over a month informs understanding of costs, maintenance, process control, and pretreatment strategies to prevent performance degradation. The large data set under variable influent conditions generated in this study can support validation of future process models. By providing evidence for robust operation under relevant process conditions, this work advances ECS toward technology readiness level 5 (i.e., a laboratory-scale system in a simulated operational environment) as defined by the National Aeronautics and Space Administration and the Department of Defense.[26,43,44] Our long-term demonstration of ECS treating about half of the volume of urine excreted per person each day[45] will support future investigations of larger scales and other waste streams. These advancements will accelerate integration into robust treatment trains that facilitate the achievement of several United Nations Sustainable Development Goals (SDGs): provision of safe drinking water and sanitation (SDG 6), responsible consumption and production (SDG 12), and protection of water resources against pollution (SDG 14).[13,46]

2. MATERIALS AND METHODS

2.1. Electrochemical Reactors

ECS experiments were performed in a three-chambered parallel-plate reactor (Figure S1-1) constructed of three frames (internal dimensions 8 cm × 8 cm × 1.9 cm) compressed between two square plates (dimensions 18 cm × 18 cm × 1.9 cm). Buna-N rubber gaskets (Grainger, Lake Forest, IL) were used to separate all of the reactor components and prevent leaks. Chambers 1 and 2 were separated by a cation exchange membrane (CEM; FumaTech Fumasep FKS-50, Fuel Cell Store, Bryan, TX). Chambers 2 and 3 were separated by a membrane facilitating ammonia transport. Chamber 1 contained a dimensionally stable titanium-based anode (64 cm^2 geometric area). Chamber 2 contained a 304L stainless steel mesh cathode (64 cm^2 geometric area, 40 mesh, 0.425 mm opening, 190 μm wire diameter, 42% open area, Yikai Industrial Scientific, Shanghai, China) with a 304 stainless steel current collector (KC Sheetmetal, San Jose, CA). The cathode was used as the working electrode, and the anode was used as the counter electrode and reference electrode to facilitate continuous monitoring of the full-cell potential. We operated the reactor galvanostatically (i.e., chronopotentiometrically, CP), controlling the rate of reaction at the working electrode by maintaining a constant current density (Interface 1010E potentiostat, Gamry Instruments, Warminster, PA). Because we did not need to precisely measure or control the interfacial potential across the working electrode−electrolyte interface, a two-electrode system without a separate reference electrode was sufficient.[47] Masterflex peristaltic pumps (VWR International, Radnor, PA) controlled the flow into and out of reactors.

The anode and the ammonia-transporting membrane between Chambers 2 and 3 varied between experiments. The anode used in Chamber 1 was either a titanium mesh electrode coated with IrO_2−Ta_2O_5 mixed-metal oxide (Magneto Special Anodes, Schiedam, The Netherlands) for batch ECS experiments (Section 2.2) or a titanium mesh electrode coated with IrO_2 mixed-metal oxide (Optimum

https://doi.org/10.1021/acsenvironau.3c00058
ACS Environ. Au 2024, 4, 89−105

Anode Technologies, Camarillo, CA) for continuous ECS experiments (Sections 2.4 and 2.6). The ammonia-transporting membrane material varied depending on experiment duration because membrane wetting occurred during preliminary long-term experiments. Specifically, a polyethylene hydrophobic membrane (Aquastill, Sittard, The Netherlands) was used for the batch experiments with different wastewaters (Section 2.2) and for the continuous experiments with varying influent urine composition (Section 2.6). For the long-term continuous experiments (Section 2.4), we used a wetting-resistant omniphobic acrylic copolymer membrane cast on a nonwoven nylon support (Versapor RC450, Pall Corporation, Port Washington, NY). For continuous experiments discussed in Sections 2.4 and 2.6, the ammonia-transporting membranes were framed with polyethylene tape (VWR International, Radnor, PA) to protect them from contact with rubber gaskets; framing with tape resulted in about 43% lower active membrane area for ammonia-transporting membranes compared with the CEM (Figure S1-2).

2.2. Feasibility of Treating Multiple Wastewaters

Triplicate batch ECS experiments (Figure S1-3A) were conducted for six different wastewaters, including fecal sludge treatment plant (FSTP) effluent, reverse osmosis concentrate from full advanced treatment of municipal wastewater, anaerobically treated mainstream municipal wastewater, and three anaerobic digestates from solids processing at municipal wastewater treatment plants. Data from previous studies were also reported for two additional wastewaters: urine and hydrothermal liquefaction effluent.[23,24] The composition of these wastewaters is summarized in Table S1-1 with process flow diagrams illustrating the sources of these wastewaters shown in Figure S1-4. Experimental conditions (i.e., applied current density and duration) (Table S1-2) were adjusted for wastewaters based on influent TAN concentration and wastewater volume treated. Reactor chambers were recirculated at a rate of 75 mL/min. ECS performance in each wastewater was evaluated based on removal and recovery efficiency, energy required for removal and recovery, and current efficiency (all metrics defined by eqs S1-10 through S1-14 in Section S1.7.1).

2.3. Urine Collection for Continuous ECS Experiments

Urine was collected from July 3, 2021 to February 9, 2022 at Stanford University's Shriram Center with approximately equal volumetric contributions from adult male and female donors (Internal Review Board Protocol 60601). Urine was stored in a closed container at room temperature (25 °C) and allowed to hydrolyze for at least 12 months. Hydrolyzed urine contained less than 0.35 mM urea-N compared to 360 ± 14 mM TAN for long-term continuous experiments (Section 2.4) and 366 ± 2.4 mM TAN for continuous experiments with varying influent urine composition (Section 2.6), indicating complete hydrolysis. For experiments involving partially hydrolyzed urine, fresh urine was collected in closed 8-ounce containers by individuals during June and July 2023 and stored at 4 °C within 3 h of collection. To minimize urea hydrolysis while allowing aggregation of samples from multiple donors, individual containers were combined into glass bottles every 1 to 2 days and stored at 4 °C until about 1 h before use in experiments.

2.4. Continuous Long-Term Urine Treatment

Two ECS reactors operated simultaneously to treat separately collected urine (Figure S1-3B). For each reactor, influent urine (Table 1) was supplied to Chamber 1 from a 10 L container (same for both reactors) and refilled daily to minimize the headspace and potential influent ammonia volatilization. Treated effluent urine from Chamber 1 was collected in a 20 L container (separate for each reactor). For each reactor, Chamber 1 was connected to a recirculation bottle initially containing 250 mL of acidified urine (pH 2.8, adjusted with H_2SO_4) to limit foaming in the reactor during early operation, likely caused by urine surfactants and bicarbonate neutralization. Chamber 2 was connected to a recirculation bottle containing 250 mL of 0.1 M NaCl, and this solution was replaced if its volume was low when the CEM was replaced (Section 3.2.1). Chamber 3 was connected to a recirculation bottle containing 500 mL of 1 M H_2SO_4. Sulfuric acid was chosen as the absorbent because it facilitated near-complete TAN recovery in previous studies.[22,23,25] The H_2SO_4 concentration was chosen to allow several days of operation before the solution was neutralized by recovered TAN and required replacement to continue providing an acidic sink that facilitates TAN recovery. Each chamber was recirculated at 59 mL/min. Influent and effluent urine were pumped at approximately 0.5 mL/min, equivalent to a hydraulic residence time (HRT) of about 4 h (eq S1-1), to achieve at least 80% removal efficiency (Figure S1-5, Section S1.3). Samples were collected from influent urine, effluent urine, combined effluent from each reactor, and all three ECS chambers at 4 and 8 h (i.e., every HRT initially) and then daily starting at 24 h. The duplicate reactors were operated for 35 and 37 days. Performance metrics (removal and recovery efficiency, energy required for removal and recovery, product purity, energy consumption per recovered product batch, and removal and recovery flux) were calculated (eqs S1-15 through S1-24 in Section S1.7.2).

Table 1. Influent Urine Characteristics for Long-Term Continuous Electrochemical Stripping (ECS) Treatment[a]

Urine	
TAN (mg/L)	5,040 ± 200
Cations (mg/L)	
Na^+	1,620 ± 81
K^+	1,640 ± 110
Mg^{2+}	1.19 ± 0.64
Ca^{2+}	11.0 ± 10
Anions (mg/L)	
SO_4^{2-}	740 ± 120
Cl^-	2,300 ± 380
PO_4^{3-}	640 ± 110
Other	
pH	9.25 ± 0.10
Electrical conductivity (mS/cm)	30.6 ± 8.7
COD (mg/L)	4,040 ± 250
Total inorganic carbon (TIC, mg/L)	1,990 ± 88
Total organic carbon (TOC, mg/L)	1,550 ± 150

[a] NO_3^-, NO_2^-, Br^-, and F^- were not detected. Urine compositions reported in literature vary, but the composition reported here falls within reported ranges.[4,45,48] Resuspension of precipitated salts during refilling of the influent container could cause variable Ca^{2+} concentration.

2.5. Electrochemical Monitoring of Long-Term Urine Treatment

Two electrochemical monitoring measurements, electrochemical impedance spectroscopy (EIS) and fast chronopotentiometry (CP), were performed daily for the first 14 days of the long-term experiment and every 2−4 days for the remainder. When performing electrochemical monitoring, we paused ECS operation and recirculated the solutions for 5 min to disperse dissolved hydrogen and oxygen. We then stopped recirculation, completed both electrochemical measurements, and resumed recirculation and ECS operation. Gamry Interface 1010E potentiostats were used for electrochemical monitoring measurements.

Galvanostatic EIS was used to determine the contributions of membranes and solutions to the overall resistance. This measurement was conducted when ECS operation was paused and repeated with the same settings about 2 min after ECS operation resumed. Platinum wire electrodes (0.5-mm diameter, Thermo Scientific, Waltham, MA) were immersed into the middle of Chambers 1 and 2 (Figure S1-6A), with the electrode in Chamber 2 acting as the working electrode and the electrode in Chamber 1 acting as the counter and reference electrode. An alternating current with a frequency of 0.01 Hz to 0.1 MHz and an amplitude of 0.1 rms mA (root mean squared; i.e., 0.14 mA peak current) was applied, and six measurements per decade were taken. The *x*-intercept of Nyquist plots, representing the total

https://doi.org/10.1021/acsenvironau.3c00058
ACS Environ. Au 2024, 4, 89−105

membrane and solution resistance,[49,50] was determined for each measurement. If the data crossed the x-axis, the x-intercept was interpolated using a linear fit defined by the two points closest to and on opposite sides of the x-axis. If the data did not cross the x-axis, the x-intercept was extrapolated by using a linear fit to the two points closest to and above the x-axis. To isolate the contribution of membrane resistance to total resistance, we subtracted solution resistance (calculated from Chamber 1 and 2 solution conductivities) and resistance of electrical patch cords from the total measured resistance (eqs S1-2 through S1-6, Section S1.4).

Fast CP was conducted to study changes in the mechanisms of ion transport that can be associated with membrane fouling. Current densities of 10 and 2 mA/cm^2 (i.e., operational ECS current density and a current density similar to that applied during CP in other ion exchange membrane investigations[51,52]) were applied for 60 s, and full-cell voltage was measured every 0.01 s. We used the stainless steel cathode as the working electrode and the anode as the counter and reference electrodes (Figure S1-6B). The observed full-cell voltage was plotted over time, and two values were extracted from the curves: the initial voltage drop (full-cell voltage at 0.01 s) and the transition time (first inflection point).

2.6. Impacts of Urine Collection Factors on Performance

To investigate the impact of influent urine composition on ECS performance, we investigated three factors that vary with urine collection and storage procedures: (1) dilution of urine with flush water, (2) extent of divalent cation precipitation, and (3) degree of urea hydrolysis. Solutions in each chamber, recirculation flow rate, and influent and effluent flow rates were identical to those used in continuous long-term experiments (Section 2.4). Influent urine was supplied from a 2 or 10 L container, and treated effluent urine was collected in a 2 or 10 L container. Duplicate or triplicate 48 h continuous ECS experiments (Figure S1-3B) were conducted for each influent (Tables S1-3 through S1-5). Samples were collected from each chamber and the effluent at 0, 16, 20, 24, 36, 40, 44, and 48 h to capture multiple data points during transient and steady-state periods. Influent samples were collected at 0, 24, and 48 h to verify that influent composition remained consistent throughout each experiment. Performance metrics (removal and recovery efficiency, energy required for removal and recovery, current efficiency, and removal and recovery flux) were calculated (eqs S1-15, S1-17 through S1-19, and S1-22 through S1-24 in Section S1.7.2).

2.7. Membrane Characterization

After removal from the reactor, CEMs and omniphobic membranes were stored and dried in closed Petri dishes for 2 to 4 months before characterization. Scanning electron microscopy (SEM, Thermo Fisher Scientific Apreo S LoVac microscope) and energy-dispersive X-ray spectroscopy (EDS, Bruker Quantax XFlash 6|60 EDS detector) were used to understand the morphology and elemental distribution of the foulants on the membrane surface.[34,53−63] Membrane samples were mounted on aluminum pin stubs and sputter-coated with gold to improve the imaging surface conductivity. The SEM images and EDS elemental maps (C, O, Na, K, Ca, Mg, P, and S) were acquired at 12 kV and 50 pA. EDS data were collected at two points on each membrane sample. Functional groups of the foulants were analyzed using Fourier transform infrared spectroscopy (FTIR, Thermo Fisher Scientific Nicolet iN10) with an attenuated total reflection (ATR) accessory.[34,55,57−59,62,64] Spectra were obtained by averaging 128 scans with a wavenumber resolution of 4.0 cm^{-1} in the range of 680−2000 cm^{-1}. A high-sensitivity liquid nitrogen-cooled detector was used to distinguish small features due to a high background signal from the virgin membrane. ATR-FTIR data were collected at two or more points on each membrane, but we only showed multiple spectra if different features were detected at different points (Section 3.2.4).

Potentiostatic EIS was used to determine the ionic conductivity of the CEM.[65−67] For the virgin CEM and each used CEM, four samples were cut slightly larger than the circular electrode (2 cm diameter) in the sample holder and equilibrated with 0.1 M NaCl solution overnight prior to measurement. Stacks consisting of 1, 2, and 3 samples were placed into a sample holder (BioLogic CESH-e, Seyssinet-Pariset, France) and compressed to allow through-plane measurement. Using a VMP potentiostat and EC-Lab software (BioLogic, Seyssinet-Pariset, France), an oscillating potential of 10 mV was applied with a frequency of 100 Hz to 3 MHz, and ten measurements per decade were taken for two replicate CEM stacks. Open- and short-circuit compensation tests were conducted to characterize the resistance contributions from the CESH-e device and wiring, and EIS spectra were corrected with the compensations. The thickness of each membrane stack was measured at five positions by using a digital micrometer (Mitutoyo America Corporation IP65, Aurora, IL). The x-intercept of the Nyquist plot was taken as the total ohmic resistance of the membrane, membrane−electrode interfaces, and electrolyte−surface interfaces. The measured area resistance, determined as the product of the electrode area and the measured total resistance, was plotted against the stack thickness, and ionic conductivity was calculated from the slope of a linear fit (eqs S1-7 through S1-9, Section S1.6).

2.8. Chemical Analyses

Sample pH was measured with a pH meter (FiveEasy F20 or SevenDirect SD20, Mettler Toledo, Columbus, OH) and sample conductivity was measured with a pH/conductivity meter (SevenDirect SD23, Mettler Toledo, Columbus, OH). TAN concentrations were determined by the indophenol method using flow-injection analysis (AA500 AutoAnalyzer, SEAL Analytical, Mequon, WI). A Dionex ICS-6000 was used to determine cation concentrations (IonPac SCS1 column, unsuppressed, 4 mM tartaric acid/2 mM oxalic acid eluent, 1.0 mL/min, 30 °C, Thermo Scientific, Waltham, MA) and anion concentrations (IonPac AS22-4 μm column, suppressed, 4.5 mM Na_2CO_3/1.4 mM $NaHCO_3$ eluent, 1.0 mL/min, 30 °C, Thermo Scientific, Waltham, MA). Chemical oxygen demand (COD) was determined colorimetrically by Hach Method 8000 using high-range (0−1,500 mg/L) reagent kits (CHEMetrics, Midland, VA) with a DRB200 digital reactor block and a DR1900 portable spectrophotometer (Hach Company, Loveland, Colorado). Total organic and inorganic carbon (TOC and TIC) were measured using a Shimadzu TOC-L autoanalyzer (Shimadzu Scientific Instruments, Inc., Columbia, MD).

2.9. Preliminary Cost Assessment

Capital costs for the ECS reactor (Table S1-6) were determined based on the reactor components for the long-term continuous experiment (Section 2.1). Operating costs (Table S1-7) accounted for electricity consumption by ECS and associated pumps, chemical inputs for periodic replacement of Chamber 2 and 3 solutions, and periodic replacement of key components (anode, cathode, CEM, and ammonia-transporting membrane). The cost of recovering ammonia or net present value (NPV) was calculated using eq 1:

$$\mathrm{NPV} = \sum_{n=0}^{t} \frac{R_n}{(1+r)^n} = \sum_{n=0}^{t} \frac{R_{\mathrm{PV}}(1+i)^n}{(1+r)^n} \quad (1)$$

where R_n is the cash flow (i.e., costs) during time period n, R_{PV} is the present value of a cash flow, r is the discount rate (10%) used to convert cash flows during time period n to present value, i is the interest rate (3%) used to determine cash flows during time period n based on the present value of cash flows, and t is the time period for the cost assessment (20 years). Operating costs of ECS were compared to those of other TAN removal and recovery processes.

3. RESULTS AND DISCUSSION

3.1. Feasibility of Treating Multiple Wastewaters

Batch experiments demonstrated the applicability of ECS to multiple wastewaters with varying characteristics (Table S1-1). ECS achieved greater than 90% TAN removal in all wastewaters tested in this and previous studies, including urine, hydrothermal liquefaction effluent, FSTP effluent, reverse osmosis concentrate, anaerobically treated mainstream wastewater, and three anaerobic digestates from solid

https://doi.org/10.1021/acsenvironau.3c00058
ACS Environ. Au 2024, 4, 89−105

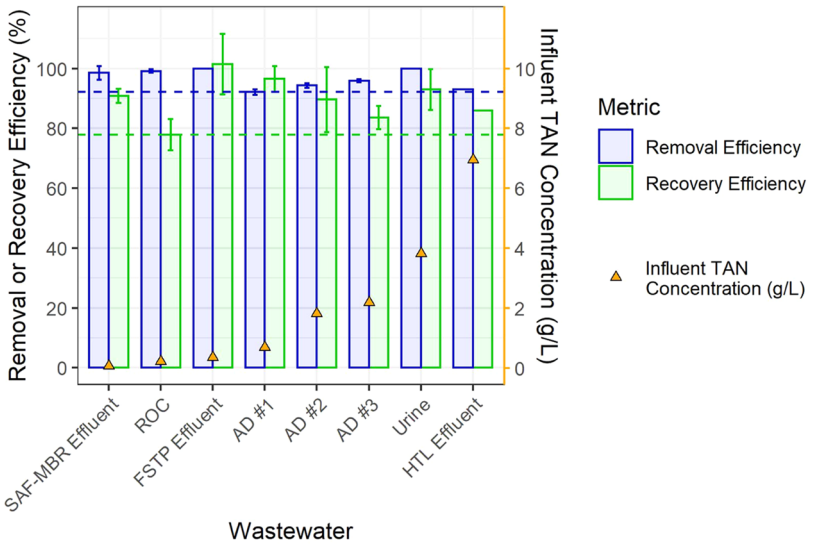

Figure 1. Total ammonia nitrogen (TAN) removal and recovery efficiency in multiple wastewaters with TAN concentrations (shown on the right axis) varying across 2 orders of magnitude. Wastewaters are arranged in order of increasing TAN concentrations from left to right. SAF-MBR effluent is a staged anaerobic fluidized membrane bioreactor effluent; ROC is reverse osmosis concentrate; FSTP effluent is fecal sludge treatment plant effluent; AD is anaerobic digestate; and HTL effluent is hydrothermal liquefaction effluent. All wastewaters were generated during the treatment of municipal wastewater with process flow diagrams shown in Figure S1-4. Dashed horizontal lines indicate the lowest removal (blue) and recovery (green) efficiencies observed across the wastewaters. Data for urine and HTL effluent are taken from previous ECS studies;[23,24] experiments for all other wastewaters were performed in the current study. Statistical analysis of differences between removal and recovery metrics is shown in Table S2-1.

processing at municipal wastewater treatment plants. ECS also recovered greater than 75% of TAN in all wastewaters tested and greater than 80% of TAN in all wastewaters, except reverse osmosis concentrate (Figure 1). Reverse osmosis concentrate exhibited three to 30 times higher divalent cation (Mg^{2+}, Ca^{2+}) concentrations than other wastewaters (Table S1-1). Under basic conditions in Chamber 2, these ions precipitate (e.g., as phosphate and carbonate salts[68,69]) and could deposit on membrane surfaces, interfering with TAN recovery.

Energy consumption for TAN removal and recovery ranged from 49.2 to 606 MJ/kg N for most wastewaters investigated (Figure S2-1), except for FSTP effluent, which required about 2,900 MJ/kg N. The high energy consumption for FSTP effluent can be attributed to a difference in reactor configuration and selection of current density (Table S1-2). For FSTP effluent, electrodes were placed at opposite ends of reactor chambers instead of immediately adjacent to the CEM (the case for all other wastewaters tested in this study), which caused solution resistance to contribute more significantly to the full-cell potential and energy demand. Moreover, a relatively high current density of 100 A/m^2 was used as in a previous study on urine treatment[23] despite the low conductivity of FSTP effluent (4.5 vs 24.7 mS/cm for urine). The resulting greater ratio of current density to wastewater conductivity (Figure S2-2) compared to other wastewaters contributed to the greater energy input required for FSTP effluent. These results illustrate the importance of tuning the reactor configuration and operating conditions to influent composition.

We demonstrated a proof-of-concept for applying ECS to various wastewaters with operating conditions selected based only on influent wastewater volume and TAN concentration. Further optimization of the operating parameters could reduce energy consumption. Current density normalized to TAN mass introduced in the influent, removed from the influent, or recovered to Chamber 3 (Figure S2-3A) reflected trends in energy consumption across wastewaters, as did the charge passed normalized to TAN mass removed and the current efficiency (Figure S2-3B). Researchers previously identified the load ratio (i.e., current density normalized to TAN loading rate) as a predictive parameter for removal efficiency and energy consumption for continuous electrodialysis−membrane stripping;[70] thus, load ratio could also help optimize batch operating conditions for energy efficiency based on influent composition.

3.2. Robustness during Continuous Urine Treatment

3.2.1. Nutrient Removal and Recovery Performance during Long-Term Operation. We focused long-term evaluation on urine treatment because urine is a high-conductivity, high-TAN waste stream amenable to energy-efficient electrochemical treatment[7,23,71] and because source separation of urine could provide many wastewater treatment benefits.[72−76] When treating influent urine containing 5,050 ± 210 mg/L TAN for over 30 days, ECS achieved consistent steady-state removal and recovery efficiencies of 83.4 ± 1.5 and 73.0 ± 2.9%, respectively (Figure 2A), after an initial transient start-up phase (Figures S2-4 through S2-7). Most electrochemical nutrient recovery technologies, except bioelectrochemical systems, have been operated for much shorter times on the order of days.[27,29]

Both ECS reactors achieved reproducible TAN recovery, with each reactor generating eight batches of ammonium sulfate solution (product TAN concentrations in Figures 2A and S2-8). Product TAN concentration rose steadily until the initially supplied 1 M H_2SO_4 was neutralized (pH values in Figures 2A and S2-8), reaching a final pH of 8.59 ± 0.47 across both reactors. The products exhibited consistent TAN concentrations of 1.49 ± 0.15 M (20.9 ± 2.0 g/L) TAN across the eight batches recovered by each reactor (i.e., 16 batches total), which was slightly lower than commercial

https://doi.org/10.1021/acsenvironau.3c00058
ACS Environ. Au 2024, 4, 89−105

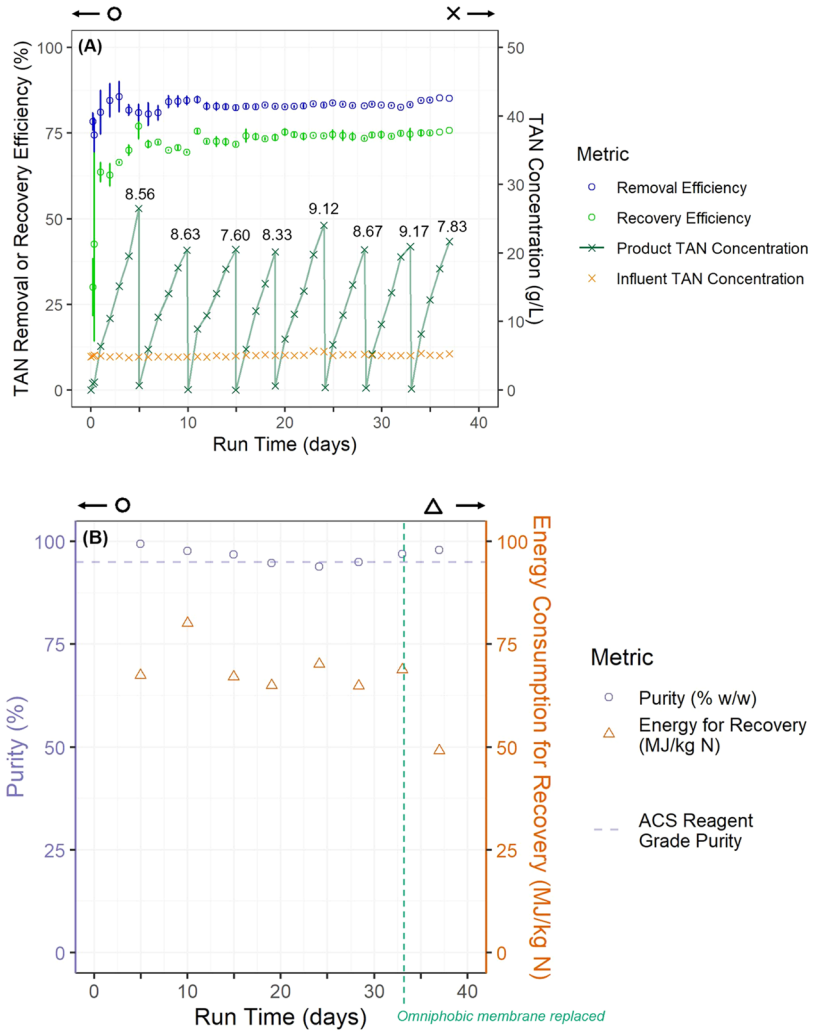

Figure 2. (A) Long-term performance metrics for electrochemical stripping (ECS). Daily influent TAN concentration for both reactors and average cumulative removal and recovery efficiency achieved by two reactors are shown along with the product TAN concentration achieved by one reactor (Reactor A). The product TAN concentration profile for Reactor B is shown in Figure S2-8B. Final product batch pH values are noted at each peak in the product TAN concentration profile, which corresponds to the time of trap solution replacement. (B) Purity of recovered product batches and energy required for generating each batch for Reactor A. Analogous data for Reactor B are shown in Figure S2-10. The vertical green line indicates replacement of the omniphobic membrane.

ammonium sulfate fertilizers (28.4 g/L TAN)[77] but similar to concentrations recovered from synthetic anaerobic digestate by an electrodialysis−membrane stripping system.[77] Therefore, ECS repeatably achieved a concentration factor of 4.1 ± 0.4 for the neutral product compared to the average influent concentration. In total, Reactors A and B recovered 107 and 103 g TAN from 27.8 and 26.4 L of urine over the entire operating period, respectively (Figure S2-9).

Implementation of ECS requires the recovery of a high-quality product. When considering anionic and cationic impurities measured by ion chromatography (IC) (specifically Na^+, K^+, Ca^{2+}, Mg^{2+}, Cl^-, PO_4^{3-}, NO_3^-), multiple consecutive batches of recovered ammonium sulfate met ACS reagent-grade purity guidelines of 95% (w/w) (Figures 2B and S2-10).[78] In decreasing concentration (mg/L) order, K^+, Na^+, and Cl^- were detected in the recovered product. K^+ is an important mineral for plant growth[79] and, therefore, likely not a concerning contaminant for the application of recovered ammonium sulfate as a fertilizer, but Na^+ and Cl^- can contribute to increasing soil salinity, which can reduce agricultural productivity.[80] Despite some K^+ and Na^+ transfer to the product chamber, ECS was highly selective for TAN recovery; K^+ and Na^+ were removed about 1.2 times as efficiently as TAN (99% K^+ and Na^+ removal vs 83.4% TAN removal), but TAN recovery efficiency was about 91 and 66 times the recovery efficiency of Na^+ and K^+, respectively (73.0% TAN recovery vs 0.80% Na^+ recovery and 1.1% K^+ recovery). After purity fell below reagent grade, replacement of the omniphobic membrane restored product purity for Reactor A. Reactor B did not exhibit the same purity effect likely because of an undersized replacement membrane (Figure S2-11).

To investigate contaminants beyond the inorganic ions measured by IC, we quantified TOC and TIC (Figures S2-12 and S2-13). TOC and TIC were present in the products starting with the first batch, but concentrations remained approximately constant for the first four batches (20 days). For batches five through eight, the TOC concentration increased significantly, while TIC remained similar or slightly greater than for the first four batches. The increase in TOC aligned

https://doi.org/10.1021/acsenvironau.3c00058
ACS Environ. Au 2024, 4, 89−105

with the increased presence of ionic contaminants and the associated drop in purity (Figure 2B). We observed a more dramatic increase in TOC for the final batch recovered in Reactor B, which provides further evidence of an undersized replacement membrane. Organic contamination could originate from degrading polymeric membranes,[81,82] transmembrane migration of urine constituents (e.g., amino acids, pharmaceuticals), and urine contamination due to compromised CEMs.[4,83−85] Inorganic carbon contamination could originate from bicarbonate in influent urine and equilibration with atmospheric CO_2, which is highly soluble in basic solutions.[86−88] Although ECS with hydrophobic membranes showed negligible pharmaceutical migration to Chamber 3,[23] omniphobic membranes treating larger volumes of urine could have enhanced organic migration. More thorough characterization of carbon-containing constituents could prove valuable for addressing potential user concerns about product purity[89] and for informing mitigation strategies.

We evaluated electrical energy consumption for ECS throughout the long-term experiment because previous studies indicated that it was the predominant factor in overall energy demand.[23] Energy consumption for recovery was 70.1 ± 9.4 MJ/kg of N when averaged across all batches generated by both reactors (Figures 2B and S2-10). Daily evaluation of energy consumption for removal and recovery showed consistent values throughout the experiment (Figure S2-5A). From 48 h onward, average steady-state energy consumption was 61.2 ± 4.2 MJ/kg N removed and 69.6 ± 3.2 MJ/kg N recovered. These values were about twice the energy consumption (30.6 MJ/kg N removed) reported in a previous ECS study, in which only 60.6% of influent TAN was removed and 49.6% was recovered while continuously treating urine.[23] Thus, in this study, we inputted more energy (i.e., applied greater current density relative to flow rate) to achieve more complete treatment (83.4% removal and 73.0% recovery). We also compared removal/recovery efficiency and energy consumption observed in this study to values reported for other TAN removal and recovery technologies applied to urine or synthetic urine (Figure S2-14, Table S2-2). ECS achieved greater removal/recovery efficiencies than many other processes but also required more energy, further highlighting that more complete treatment (i.e., greater removal/recovery efficiency) often requires more energy. Further optimization and reactor engineering of ECS could improve ECS performance relative to other emerging urine treatment and nutrient recovery technologies and reduce ECS energy consumption toward that of Haber-Bosch ammonia synthesis (about 31.6 MJ/kg N)[90] or conventional ammonia stripping (32 MJ/kg N).[91]

3.2.2. Operation and Maintenance Tasks. O&M tasks for membrane-based and electrochemical processes are often tied to membrane fouling, which hinders stable long-term operation.[34,58] In addition to absorbent solution renewal and omniphobic membrane replacement (Section 3.2.1), lab-scale ECS operation showed that replacing failed CEMs was a major O&M task. CEMs were replaced every 5.2 ± 1.9 days (reactor A) and 8.4 ± 2.5 days (reactor B) when the effluent pH was 25% higher than the steady-state average (Figure S2-15). Although we could have continued operation longer per membrane (no decline in cumulative removal efficiency observed), we chose to replace the CEMs at the first sign of failure to ensure that removal and recovery efficiency remained stable and high. Frequently replacing the CEM also reduced contamination of Chamber 2 with urine constituents (i.e., components other than cations that we expect to transfer across the CEM), minimizing the potential for omniphobic membrane degradation and product contamination. Future work could focus on determining the upper limit of membrane lifetime instead of the upper limit of process operation explored here.

Replacing CEMs and omniphobic membranes required pausing operation, emptying the ECS reactors, and disassembling the reactors. The complexity and disruptiveness of this procedure demonstrated the need to design scaled-up reactors that are easily serviceable, for example, by facilitating membrane replacement without significant disassembly (e.g., sliding a framed membrane into the reactor), and highlights the importance of operating redundant ECS units to avoid treatment interruptions during maintenance.

3.2.3. Potential Process Monitoring Parameters. Ideal ECS monitoring parameters are (1) fast, requiring minimal interruption of treatment or allowing online measurement, and (2) inexpensive, requiring few additional parts or equipment beyond components in the ECS reactor and common at treatment plant laboratories. The following sections summarize the parameters studied for monitoring the overall process function, CEM integrity, and omniphobic membrane integrity. pH, full-cell voltage, product (Chamber 3) volume, and water flux across the omniphobic membrane were identified as promising process monitoring parameters, while *in situ* EIS, fast CP, and product conductivity require method modifications and further study to evaluate their utility as monitoring tools.

3.2.3.1. Overall: pH. Because ECS relies on pH swings to achieve TAN removal and recovery, pH is a critical monitoring parameter. TAN removal requires a low pH in Chamber 1 to facilitate the conversion of neutral NH_3 in the influent to cationic NH_4^+, which can electromigrate across the CEM. TAN recovery requires a high pH in Chamber 2 to facilitate the conversion of NH_4^+ to NH_3, which can cross the omniphobic membrane. TAN recovery also requires a low pH in Chamber 3 to facilitate the conversion of NH_3 back to NH_4^+, creating an NH_3 sink and, therefore, a persistent driving force for NH_3 diffusion from Chamber 2 to 3.

pH trends and associated reactor O&M tasks are shown in Figures 3 and S2-16. During normal operation, the effluent pH remained stable at about pH 2. When effluent pH increased toward the neutral range despite no significant changes in influent pH, we replaced the CEM, which restored the effluent pH to typical values. Therefore, effluent pH is a valuable indicator for CEM failure because it demonstrates when significant leakage of hydroxide or NH_3 occurs from Chamber 2 to Chamber 1. Hydroxide ions (OH^-) are highly mobile and can cross CEMs, particularly if membrane degradation decreases permselectivity.[92] NH_3, a small neutral molecule, can diffuse through CEMs.[83−85] Increasing effluent pH was often correlated with increasing effluent TAN concentration and decreasing instantaneous removal efficiency (Figure S2-17). Therefore, online pH monitoring could be a valuable indicator for deterioration of removal performance, allowing quicker responses to diminished removal than offline TAN analysis.

Chamber 2 pH generally remained between pH 13 and 14, suggesting that damage to the CEM or omniphobic membrane was not sufficient to allow acid leakage into Chamber 2. However, catastrophic failure of the omniphobic membrane

https://doi.org/10.1021/acsenvironau.3c00058
ACS Environ. Au 2024, 4, 89−105

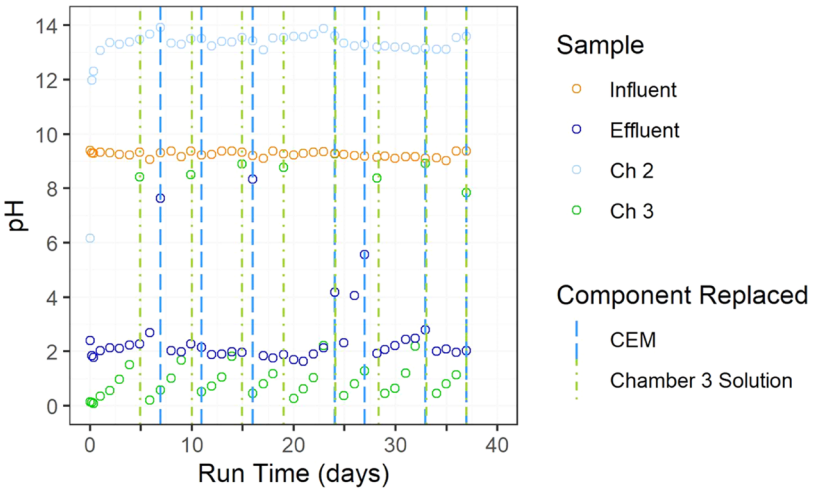

Figure 3. pH values in influent, effluent, and Chambers 2 and 3 over time with replacement of the cation exchange membrane (CEM, vertical blue lines) and replacement of exhausted Chamber 3 solution (vertical green lines) indicated for Reactor A. Data for Reactor B are shown in Figure S2-16.

could likely be detected by a pH decrease in Chamber 2. Chamber 3 pH increased periodically every 4 to 5 days when TAN absorption neutralized the sulfuric acid in Chamber 3; thus, pH is an essential indicator for replacing Chamber 3 solution to continuously recover TAN. pH probes, which are readily available, could be integrated into ECS reactors, enabling real-time monitoring that signals the need for multiple O&M tasks.

3.2.3.2. Cation Exchange Membrane: Operational Full-Cell Voltage, EIS, and Fast CP. The full-cell voltage for ECS can reflect changes in the CEM, electrodes, and solution composition. We observed a rapid increase in full-cell voltage magnitude upon resuming operation after performing process monitoring measurements or routine maintenance tasks that required pausing the experiment (Figure S2-18). This pattern reflects the ohmic potential drop associated with the membrane and surrounding electrolyte, the rapid emergence of strong concentration polarization when an overlimiting current was applied, and the Nernstian shift for the pH-affected oxygen evolution and hydrogen evolution reactions.[51,52,93,94] In general, the magnitude of full-cell voltage increased over the course of each CEM's use, suggesting that fouling contributed to increased membrane resistance. The degree of change varied across the reactors and membranes, but these differences could not be explained by CEM characterization (Section 3.2.4).

In situ EIS showed no consistent trend in the measured membrane or total resistance over the time for which each CEM was used (Figures S2-19 through S2-22, Table S2-3). Nevertheless, the similarity of results of non-operational and operational *in situ* EIS measurements suggests the feasibility of online EIS monitoring without interruption of ECS treatment. We determined the ionic conductivity of each membrane after removal from the reactor using a higher fidelity, more controlled EIS measurement method compared with our *in situ* method. The ionic conductivity of the used membranes was significantly lower than that of the virgin membrane, and ionic conductivity generally decreased as the duration of installation increased (Figures S2-23 through S2-25). These results suggest that fouling hindered ion movement through the CEM. We expect that *in situ* EIS monitoring can be more informative if the setup more closely mimics the setup used for offline ionic conductivity measurement (e.g., planar electrodes in direct contact with the membrane[95,96]).

From fast CP, we can extract two informative parameters: an initial voltage drop (ohmic potential drop caused by membrane and electrolytes without concentration polarization)[51,52,93,94] and transition times (indicating a change in ion transport mechanisms).[93,97,98] For each membrane used in each reactor, we observed a weak increasing trend in initial voltage drop over time for fast CP at 2 mA/cm^2 but no temporal trend for fast CP at 10 mA/cm^2 (Figure S2-26). These results suggest that during the time scales for which CEMs were used in this study (5−8 days), membrane degradation and fouling were insufficient to significantly affect initial potential drops during fast CP.[52] For most of the fast CP data collected during our experiments, no clear transition times could be identified (Figures S2-27 through S2-31), which could be related to the heterogeneity of the CEM, the current densities chosen, or the electrode configuration (Section S2.2.2). While we used a two-electrode configuration for simplicity and cost reduction, conducting CP at lower but still overlimiting current densities using a four-electrode configuration[93] could improve the identification of transition times and support the development of more informative CP-based monitoring techniques.

3.2.3.3. Omniphobic Membrane: Water Flux, TAN Flux, and Product Conductivity. Intact omniphobic membranes facilitate diffusion of NH_3 and potentially other small, uncharged, gaseous species (e.g., water vapor) from Chamber 2 to 3. However, wetted omniphobic membranes allow liquid water transfer and diffusion of dissolved charged species between Chambers 2 and 3, decreasing product purity.[99,100] During long-term operation, water flux for Reactor B increased steadily, suggesting increasing omniphobic membrane wetting (Figure S2-32); water flux for Reactor A was generally lower, explaining this reactor's greater product purity (Figures 2B and S2-10). Therefore, product (Chamber 3) volume and water flux could be informative monitoring parameters, but further investigation of the relationship between these metrics and product quality is needed to identify threshold values indicating omniphobic membrane issues.

The decreasing flux of desired species over time indicates fouling of omniphobic and hydrophobic membranes.[55,101,102]

https://doi.org/10.1021/acsenvironau.3c00058
ACS Environ. Au 2024, 4, 89−105

TAN recovery flux across the omniphobic membrane remained stable at 27.5 ± 3.8 g/m^2/h for Reactor A and 28.1 ± 0.86 g/m^2/h for Reactor B at 48 h onward (Figure S2-33, Table S2-4). The TAN recovery rate also remained stable throughout the entire experiment at 0.117 ± 0.0041 g/h (Reactor A) and 0.118 ± 0.0035 g/h (Reactor B), with little effect from omniphobic membrane replacement. Consistent TAN recovery flux and rate suggested that omniphobic membrane fouling did not interfere with TAN transport from Chamber 2 to Chamber 3, but increasing membrane wetting could have compensated for fouling-induced hindered transport.

Distillate conductivity has been proposed as an indicator of wetting for hydrophobic membranes in membrane distillation.[54,99,103] We observed a reproducible decrease in Chamber 3 conductivity for both reactors from fresh H_2SO_4 solution to final recovered batches of $(NH_4)_2SO_4$ solution (Figure S2-34), which was mainly driven by TAN chemistry: when NH_3 is absorbed in Chamber 3, a proton is consumed to generate NH_4^+, which has an ionic conductivity almost 5 times lower than that of protons.[104] Water transfer across the omniphobic membrane also diluted the product and contributed to decreasing conductivity; however, other charged species transfer (e.g., K^+, Na^+) would have increased conductivity. Based on these results, conductivity is not sensitive enough to be used as an indicator of product purity decreasing below a 95% threshold (i.e., below ACS reagent grade). However, the conductivities of simulated products with varying purities (Figure S2-35, Table S2-5) illustrated a near-linear relationship between conductivity and purity when neglecting water transfer across the omniphobic membrane. Further study is needed to understand the competing impacts of water and ion transfer on conductivity and to evaluate the effectiveness of conductivity as an indicator of more dramatic changes in purity.

3.2.4. Cation Exchange and Omniphobic Membrane Failure and Characterization. Because CEM failure (based on Chamber 1 effluent pH) occurred multiple times throughout our long-term experiments, CEM lifetime and failure mechanisms warrant further discussion. The duration for which CEMs are installed in reactors is a common way of reporting lifetime throughout literature despite variations in operating conditions (e.g., current density, influent flow rate).[52,105−108] Therefore, we described the membrane lifetime with duration of installation and several other metrics related to operation time and treatment achieved (Table S2-6). Because product purity decreased throughout the long-term experiment, we characterized the omniphobic membranes used for 33 and 31 days in Reactors A and B, respectively, to identify fouling that may have contributed to diminishing membrane performance.

SEM-EDS and ATR-FTIR indicated both organic and inorganic fouling on CEMs after use in ECS (Figures S2-36 through S2-38, Table S2-7 in Section S2.2.4), while only inorganic scaling was detected for omniphobic membranes (Figures S2-39 and S2-40, Table S2-8 in Section S2.2.4). Carboxylic acids and amides were detected on many CEMs, demonstrating the presence of organic foulants, possibly including amino acids, organic acids, creatinine, caffeine, pharmaceuticals, and various carbohydrates present in urine.[4,85] Scaling mainly consisted of calcium and magnesium carbonates and phosphates for both CEMs and omniphobic membranes. Variations in composition within and across membranes (especially CEMs) indicated heterogeneous membrane fouling and reflected differences in the composition of the Chamber 2 solution (Figure S2-41). These results demonstrate the need to mitigate organic and inorganic fouling to maintain membrane functionality and ECS performance stability. Potential mitigation strategies include using alternative membrane materials,[109,110] modifying reactor architectures to protect membranes from harsh conditions,[16,111−116] implementing tailored cleaning protocols,[58,103,108,117−123] and incorporating urine pre-treatment.

3.3. Impacts of Urine Collection Factors on ECS Performance

Understanding the impacts of upstream urine collection and treatment practices on ECS operation can inform the infrastructure required for implementing ECS. We considered three influent urine composition factors in 48 h continuous experiments: dilution with flush water, precipitation of divalent cations, and extent of hydrolysis. Flush water dilution relates to urine collection methods; divalent precipitation and hydrolysis relate to storage time and conditions. Despite significant differences in the composition of influent urine based on these three factors, ECS achieved more than 69% removal and 65% recovery for all conditions (Figures 4 and S2-42). Further interrogating the relationship between ECS performance and influent conditions can inform the design and operation of complete urine collection and treatment systems.

We studied three dilution factors: no dilution (i.e., unmodified urine); dilution in the case of an ultralow-flush, urine-separating toilet (i.e., 2 times dilution); and dilution in the case of a standard urinal (i.e., 20 times dilution). A positive correlation between removal/recovery efficiencies and urine dilution was observed, but not all differences between conditions were statistically significant (Figures 4, S2-42, Tables S2-9 and S2-10). At greater dilutions, more complete treatment was achieved because HRT and current density remained constant at lower TAN concentrations. However, the additional treatment entailed greater energy consumption due to the lower conductivity of diluted influent urine, which caused a greater full-cell voltage. The standard-flush influent condition (1,950 ± 290 MJ/kg N recovered) resulted in about 30 times greater energy consumption than for unmodified urine (64.7 ± 1.1 MJ/kg N), and the ultralow-flush condition (126 ± 2.7 MJ/kg N) required almost twice as much energy as unmodified urine. The drastic increase in energy consumption and declining current efficiency (Figure S2-43) with increasing urine dilution highlight the importance of limiting flush water for energy-efficient ECS and tailoring operating conditions to influent composition and treatment goals.

Urine hydrolysis reduces the concentration of divalent cations (Mg^{2+} and Ca^{2+}) due to the precipitation of struvite, calcium phosphate (e.g., hydroxyapatite), and calcium carbonate at increasing pH values.[68,69] To reflect the varied precipitation of divalent cations, we conducted experiments with complete precipitation (i.e., unmodified urine), 50% precipitation (i.e., hydrolyzed urine amended with 2.35 mM Ca^{2+} and 2.05 mM Mg^{2+}),[4] and no precipitation (i.e., hydrolyzed urine amended with 4.7 mM Ca^{2+} and 4.1 mM Mg^{2+})[4] relative to fresh urine concentrations. We observed similar removal efficiencies (79−81%), removal fluxes (6.5−7.7 mg/m^2/s), and energy consumption for removal (54−61 MJ/kg N) for all conditions (Figures 4, S2-42, and S2-44, Tables S2-9 and S2-10). The lack of significant differences between conditions and the observed maximum current

https://doi.org/10.1021/acsenvironau.3c00058
ACS Environ. Au 2024, 4, 89−105

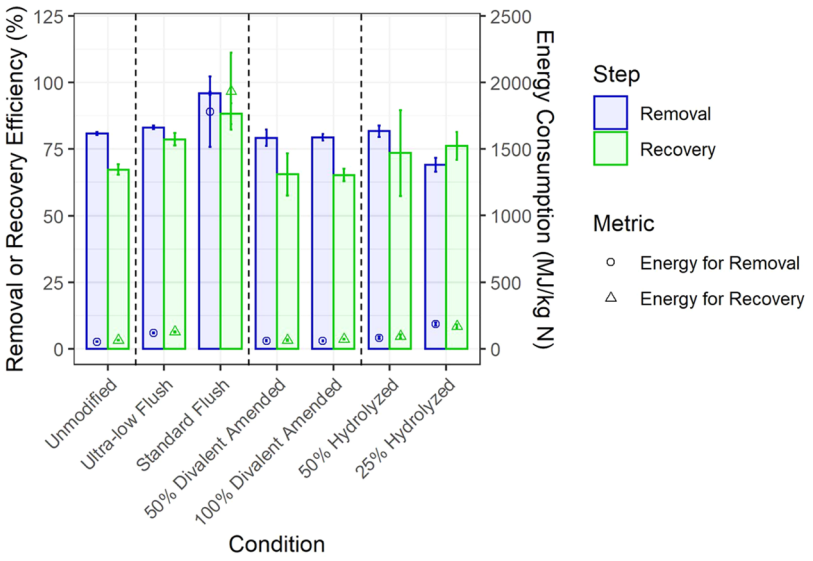

Figure 4. Total ammonia nitrogen (TAN) removal and recovery efficiency and energy consumption for electrochemical stripping (ECS) treating urine with different degrees of dilution, divalent precipitation, and hydrolysis. Black vertical lines separate the conditions tested for each of the three factors. A version of this plot with an expanded right *y*-axis is shown in Figure S2-42. The results of statistical analysis are shown in Tables S2-9 and S2-10.

efficiency at 50% amended influent (Figure S2-43) suggested a trade-off between phenomena impacting TAN removal. Divalent cations compete with NH_4^+ transport across the CEM,[124] but higher divalent cation concentrations in the influent and Chamber 1 can cause additional osmotic water transfer that increases NH_4^+ transfer,[125] resulting in a net neutral effect on TAN removal. For energy consumption, CEM resistance, voltage, and energy demand likely increased with increasing scaling at greater divalent cation concentrations (Figure S2-45); however, solution conductivity also increased with higher divalent cation concentrations, reducing the voltage and energy demand. Similar removal performance enabled similar recovery performance across different divalent cation concentrations. While we did not observe statistically significant impacts, divalent cations might have greater effects during longer operation due to accumulating CEM scaling, especially based on the increase in full-cell voltage observed over 48 h (Figures S2-45 and S2-46). These results motivate storing urine until complete hydrolysis and divalent cation precipitation before ECS treatment for optimal TAN recovery and further studying the long-term impacts of divalent cations.

Urine hydrolysis causes several additional compositional changes that increase conductivity and alkalinity, including rising pH and converting urea to TAN and bicarbonate.[69,126] Thus, we studied conditions reflecting different extents of hydrolysis, including completely hydrolyzed (i.e., unmodified urine), 50% hydrolyzed (i.e., 50% (v/v) fresh urine plus 50% (v/v) hydrolyzed urine), and 25% hydrolyzed (i.e., 75% (v/v) fresh urine plus 25% (v/v) hydrolyzed urine). Based on initially measured urea and TAN concentrations in partially hydrolyzed urine (Figure S2-47), the extents of hydrolysis (i.e., conversion of urea to ammonia) were 96.4 ± 23% for 50% hydrolyzed and 87.0 ± 5.7% for 25% hydrolyzed. Removal efficiencies decreased with decreasing extent of hydrolysis, and the 25% hydrolyzed case was statistically significantly different from the other two conditions. However, recovery efficiencies were similar for different extents of hydrolysis. Lower influent TAN concentrations at lower extents of hydrolysis caused greater competition between NH_4^+ and other ions (e.g., Na^+, K^+) for transfer across the CEM.[124] Energy for removal and recovery increased as the extent of hydrolysis decreased, but differences across the conditions were not statistically significant. Lower conductivity and lower influent TAN concentrations in less hydrolyzed urine likely caused protons to be more dominant charge carriers, decreasing TAN current efficiency (Figure S2-43) and increasing energy demand. These findings further motivate the storage of urine until complete hydrolysis before ECS treatment to reduce energy consumption and maximize TAN recovery.

Treating partially hydrolyzed urine in ECS enables investigation of the fate of urea in the process. We focus the discussion on the 25% hydrolyzed case because the influent composition remained stable for 48 h, unlike the 50% hydrolyzed case (Figure S2-47). Most urea exited ECS in the effluent or persisted in Chamber 1 (49.5 and 10.0%, respectively), while about 7.1% transferred to Chamber 2; urea was not detected in Chamber 3 (Figure S2-48). About 33.4% of urea mass was lost (Figures S2-48 and S2-49), suggesting urea transformation within ECS. Extreme ECS pH conditions (1.50 ± 0.19 in Chamber 1 and 13.3 ± 0.18 in Chamber 2) make enzymatic urea hydrolysis unlikely because urease is most stable and active from pH 5.5 to 9.[126−128] Chemical urea transformation could occur electrochemically in Chamber 1 and due to high pH in Chamber 2.[129] Depending on electrode materials, pH, and electrical potentials, electrochemical urea conversion can yield many different nitrogen products, such as N_2, CNO^-, NO_3^-, NO_2^-, $N_2O_2^-$, N_2O, NO_2, and TAN.[130−133] We observed a TAN recovery efficiency exceeding the TAN removal efficiency ($p = 0.0008$) (Figure 4) and a steady-state average TAN mass balance of 119%, which suggests that urea was transformed to TAN (Figure S2-49A). Accounting for both TAN and urea as nitrogen species, the steady-state total mass balance was about 87.8%, which supports that urea conversion to ammonia within ECS could account for the excess recovered TAN (Figures S2-49 and S2-50). For potential urea oxidation products, NO_2^- was below

https://doi.org/10.1021/acsenvironau.3c00058
ACS Environ. Au 2024, 4, 89−105

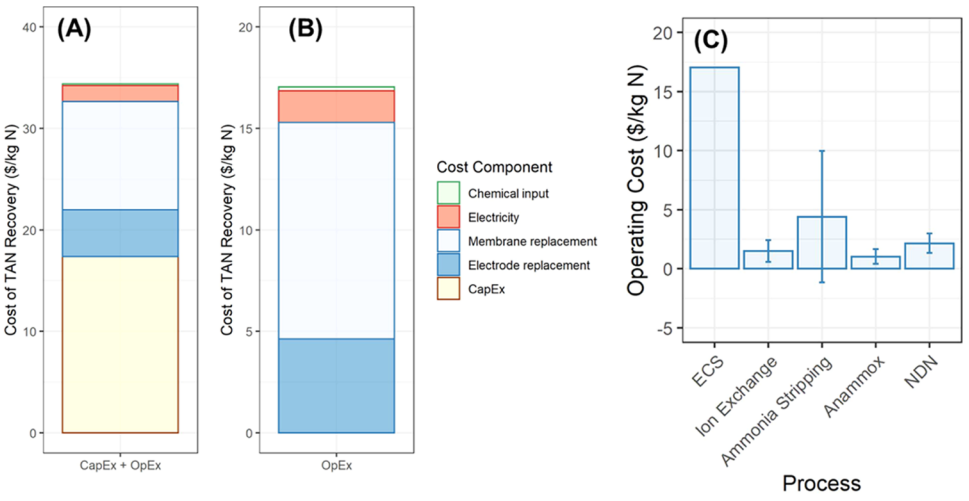

Figure 5. Life-cycle cost of total ammonia nitrogen (TAN) Recovery for electrochemical stripping (ECS) treating urine. Capital (CapEx) and operating (OpEx) costs are accounted for in panel (A), while panel (B) shows an expanded version of only operating costs. A comparison of operating costs of ECS to operating costs of other TAN removal and recovery technologies (where NDN is nitrification-denitrification) is shown in panel (C). Detailed breakdowns of capital and operating costs of ECS are shown in Figure S2-52.

detection, while NO_3^- was detected and improved the closure of the steady-state nitrogen mass balance to 89.6% (including TAN, urea, and NO_3^-). Notably, NO_3^- was also observed in the treated effluent for conditions representing different flush volumes and extents of divalent precipitation, suggesting that TAN oxidation could also be a source of effluent NO_3^- (Figure S2-51). Future experiments with gas chromatography (N_2, N_2O) and spectrophotometric methods (chloramines) could improve nitrogen mass balance closure.[23]

3.4. Preliminary Cost Assessment

To connect lab-scale investigations to practical research gaps for electrochemical processes,[15,26] we completed a preliminary cost evaluation based on the lab-scale ECS reactor and performance during long-term urine treatment. At this scale (3.1 L and 170 cm^2 for reactor without ancillary equipment) and under these operating conditions, ECS treated about half of the volume of urine excreted per person each day.[45] The process could be scaled up to serve a household (5−10× higher flow rate) and even larger buildings (100−1,000× higher flow rate). At these different scales, costs—especially capital costs—and their relative contributions could vary due to different economies of scale associated with reactor components and O&M inputs. Nevertheless, a cost estimate at the lab scale rooted in experimental results can inform scale-up investigations and design decisions.

Over a 20-year analysis time frame, ECS produced ammonium sulfate (as a 21 g/L N solution) at a cost of $34.40/kg N, which is about 16 times the North American commercial price of solid ammonium sulfate of $2.18/kg N (Figure 5A).[134] Despite the need for substantial cost reductions, ECS could help enhance global food security in the face of fertilizer price volatility[134] caused by volatile energy prices and geopolitical disruptions affecting supply chains.[135−138] Since the early 2000s, the price of ammonium sulfate has risen at rates exceeding inflation (e.g., by 2.8 times from 2001 to 2014), and even more dramatic price changes (e.g., a 2.7-time increase from January 2021 to April 2022) have occurred in recent years (Figure S2-53).[139−141] ECS implementation in regions where fertilizers are more expensive or less accessible (e.g., sub-Saharan Africa) may be more economically viable and would improve equity in fertilizer access.[39,142,143] Product diversification toward higher-value products with more applications (e.g., NH_3 vs. $(NH_4)_2SO_4$) and targeting multiple profitable uses for each chemical (e.g., $(NH_4)_2SO_4$ as a reagent is about 4−5 times more valuable than as a fertilizer)[144] could further improve process economics.

The breakdown of the ECS costs provides insights into specific cost reduction strategies. Capital costs accounted for half of the ECS life-cycle cost. Reactor housing and the anode each accounted for about 46−48% of capital costs, while the cathode, CEM, and omniphobic membrane each accounted for about 2% of capital costs (Figure S2-52, Table S1-6). Reactor housing would likely become much less expensive with scaled-up production. Exploring lower-cost but equally efficient anode materials (e.g., manganese oxybromide,[145] cobalt manganese binary oxide,[146] iron oxide-titanium dioxide[147]) could reduce capital costs, but a trade-off between capital cost and energy consumption may exist. Omniphobic membrane replacement accounted for the largest fraction (52%) of operating costs, followed by anode replacement (26%), CEM replacement (10%), and electricity (8.8%) (Figure 5B). Lifetimes of all components, including membranes and electrodes, are uncertain because different criteria for replacement can be defined and studies of component lifetime are under-represented compared to studies of other performance metrics, such as activity and selectivity.[148] Thus, the contribution of electrode and membrane replacement to operating costs may differ from this study's estimate. Multifaceted efforts are needed to enhance the economic viability of ECS, including advances in low-cost, durable materials; energy-efficient reactor configuration and operation; and recovery of high-value products.

Due to the uncertainty of several parameters that influence costs, we conducted a sensitivity analysis to determine the life-cycle cost for ECS with individual variables set to their cost-minimizing values (Table S2-11). When changing only one variable at a time (as opposed to concurrent sensitivity analyses of multiple variables), the most influential components were the costs of the anode, omniphobic membrane, and reactor housing. These variables influenced overall cost most because reactor housing and the anode dominated capital

https://doi.org/10.1021/acsenvironau.3c00058
ACS Environ. Au 2024, 4, 89−105

costs, and omniphobic membrane replacement dominated operating costs, providing additional motivation for material and reactor engineering targeting cost reduction.

Compared to four other TAN removal and recovery processes, ECS operating costs were about 4 times greater than ammonia stripping costs, 8 times greater than costs associated with the most established wastewater TAN removal process (nitrification-denitrification or NDN), and 10−15 times greater than costs of anammox and ion exchange (Figure 5C). We excluded capital costs in these comparisons because estimates varied in the scale and scope of systems considered (Table S2-12). Reported ECS operating costs are likely underestimates because we did not include labor and chemical costs associated with membrane and/or electrode cleaning (nascent and highly variable estimations exist), nor with post-treatment (e.g., for balancing pH in the ECS anode effluent). Other benefits of ECS, such as reduced chemical transport needs compared to conventional ammonia stripping and a circular nitrogen economy facilitating more equitable fertilizer access with lower environmental impacts, make process engineering to reduce capital costs, extend component lifetimes, and accelerate implementation imperative.

4. CONCLUSIONS AND IMPLICATIONS

We demonstrated that ECS can recover TAN from several waste streams (e.g., FSTP effluent, reverse osmosis concentrate, anaerobically treated wastewater) and can treat urine continuously and consistently for over a month. Future work should target reduced energy demand, reactor configurations that readily facilitate O&M tasks like membrane replacement, and investigation of membrane durability, mechanisms of degradation and failure, and cleaning for mitigating organic and inorganic fouling. Simple, inexpensive, and rapid online process monitoring remains a challenge, motivating further investigation of *in situ* electrochemical impedance spectroscopy methods that provide an indicator of CEM fouling and degradation that can be measured while ECS is operating. Moreover, multipronged approaches to improve the economic viability of ECS on a life-cycle basis should include reducing reactor component costs (especially for the anode); extending component lifetimes and reducing energy consumption through material, reactor, and process engineering; and targeting recovery of higher-value products specific to an implementation context.[18] Our study provides evidence for urine treatment as a foothold for electrochemical nutrient recovery from wastewater while demonstrating proof-of-concept for broad applicability to many wastewaters. Further research guided by our findings can accelerate the deployment of ECS at increasing scales and at more sites as the process moves along the S-curve of technology adoption toward maturity.[149] Ultimately, findings from this study support the growth of a circular nitrogen economy that fosters progress toward sanitation provision, efficient chemical production, and protection of water resources against pollution.

■ ASSOCIATED CONTENT

Supporting Information

The Supporting Information is available free of charge at https://pubs.acs.org/doi/10.1021/acsenvironau.3c00058.

Tables describing influent streams, experimental conditions, assumptions for cost estimate, and results of membrane characterization and cost estimate; equations for efficiencies, energy demand, fluxes, product purity, current efficiency, and analysis of electrochemical impedance spectroscopy data; and figures showing reactor setup, temporal trends in performance metrics and composition, membrane characterization results, and cost estimate results (PDF)

■ AUTHOR INFORMATION

Corresponding Author

William A. Tarpeh − *Department of Chemical Engineering, Stanford University, Stanford, California 94305, United States;* orcid.org/0000-0002-2950-526X; Email: wtarpeh@stanford.edu

Authors

Anna Kogler − *Department of Civil and Environmental Engineering, Stanford University, Stanford, California 94305, United States;* orcid.org/0000-0001-6594-0501

Neha Sharma − *Stanford Synchrotron Radiation Lightsource, SLAC National Accelerator Laboratory, Menlo Park, California 94205, United States; Department of Chemical Engineering, Stanford University, Stanford, California 94305, United States;* orcid.org/0000-0002-5696-2618

Diana Tiburcio − *Department of Mechanical Engineering, Temple University, Philadelphia, Pennsylvania 19122, United States*

Meili Gong − *Department of Chemical Engineering, Stanford University, Stanford, California 94305, United States*

Dean M. Miller − *Department of Chemical Engineering, Stanford University, Stanford, California 94305, United States;* orcid.org/0000-0002-7970-3475

Kindle S. Williams − *Department of Chemical Engineering, Stanford University, Stanford, California 94305, United States;* orcid.org/0000-0001-9640-7849

Xi Chen − *Department of Chemical Engineering, Stanford University, Stanford, California 94305, United States;* orcid.org/0000-0001-6404-3614

Complete contact information is available at: https://pubs.acs.org/10.1021/acsenvironau.3c00058

Author Contributions

CRediT: **Anna Kogler** conceptualization, data curation, formal analysis, investigation, methodology, project administration, validation, visualization, writing-original draft, writing-review & editing; **Neha Sharma** data curation, formal analysis, investigation, methodology, software, validation, visualization, writing-original draft, writing-review & editing; **Diana Tiburcio** data curation, formal analysis, investigation, visualization, writing-original draft; **Meili Gong** data curation, formal analysis, investigation, methodology, validation, writing-review & editing; **Dean Mackenzie Miller** formal analysis, methodology, writing-review & editing; **Kindle Shea Williams** methodology, visualization, writing-review & editing; **Xi Chen** methodology, writing-review & editing; **William A. Tarpeh** conceptualization, funding acquisition, project administration, resources, supervision, writing-review & editing.

Notes

The authors declare no competing financial interest.

■ ACKNOWLEDGMENTS

The authors thank the Tarpeh lab for productive discussions in developing this work, and particularly Matthew Liu for brainstorming on the analysis of electrochemical measurement data for process monitoring. SEM imaging and EDS mapping were performed at the Stanford Nano Shared Facilities (SNSF), supported by the National Science Foundation under award ECCS-2026822. ATR-FTIR analysis was performed at SLAC National Accelerator Laboratory with the help of Dr. Sharon Bone. TOC and TIC analyses were performed at the Environmental Measurements Facility at Stanford Doerr School of Sustainability. The project was funded by the Stanford University King Center on Global Development, the Stanford University Center for Innovation in Global Health, the Environmental Protection Agency P3 Grant (SV840417), and the Sustainability Accelerator from the Stanford Doerr School of Sustainability. Authors also acknowledge the following additional support: A.K.: Stanford University Vice Provost for Graduate Education; D.T.: Stanford Undergraduate Research Fellowship; D.M.M.: National Aeronautics and Space Administration (NASA) Space Technology Graduate Research Opportunities fellowship (Award 80NSSC22K1191); and W.A.T: Camille and Henry Dreyfus Foundation.

■ REFERENCES

(1) Dodds, W. K.; Bouska, W. W.; Eitzmann, J. L.; Pilger, T. J.; Pitts, K. L.; Riley, A. J.; Schloesser, J. T.; Thornbrugh, D. J. Eutrophication of U.S. Freshwaters: Analysis of Potential Economic Damages. *Environ. Sci. Technol.* **2009**, *43* (1), 12−19.

(2) Burow, K. R.; Nolan, B. T.; Rupert, M. G.; Dubrovsky, N. M. Nitrate in Groundwater of the United States, 1991−2003. *Environ. Sci. Technol.* **2010**, *44* (13), 4988−4997.

(3) Falconer, I. R. An Overview of Problems Caused by Toxic Blue−Green Algae (Cyanobacteria) in Drinking and Recreational Water. *Environ. Toxicol.* **1999**, *14* (1), 5−12.

(4) Udert, K. M.; Larsen, T. A.; Gujer, W. Fate of Major Compounds in Source-Separated Urine. *Water Sci. Technol.* **2006**, *54* (11−12), 413−420.

(5) van der Hoek, J.; Duijff, R.; Reinstra, O. Nitrogen Recovery from Wastewater: Possibilities, Competition with Other Resources, and Adaptation Pathways. *Sustainability* **2018**, *10* (12), 4605.

(6) Chorkendorff, I.; Niemantsverdriet, J. W. *Concepts of Modern Catalysis and Kinetics*, 1st ed.; Wiley, 2003. DOI: 10.1002/3527602658.

(7) Wald, C. The Urine Revolution: How Recycling Pee Could Help to Save the World. *Nature* **2022**, *602* (7896), 202−206.

(8) Qadir, M.; Drechsel, P.; Jiménez Cisneros, B.; Kim, Y.; Pramanik, A.; Mehta, P.; Olaniyan, O. Global and Regional Potential of Wastewater as a Water, Nutrient and Energy Source. *Nat. Resour. Forum* **2020**, *44* (1), 40−51.

(9) EPA. Biological Nutrient Removal Processes and Costs, 2007. https://19january2017snapshot.epa.gov/sites/production/files/documents/criteria_nutrient_bioremoval.pdf.

(10) US EPA. Energy Efficiency for Water Utilities, 2023. https://www.epa.gov/sustainable-water-infrastructure/energy-efficiency-water-utilities.

(11) Erisman, J. W.; Sutton, M. A.; Galloway, J.; Klimont, Z.; Winiwarter, W. How a Century of Ammonia Synthesis Changed the World. *Nat. Geosci.* **2008**, *1* (10), 636−639.

(12) Kyriakou, V.; Garagounis, I.; Vourros, A.; Vasileiou, E.; Stoukides, M. An Electrochemical Haber-Bosch Process. *Joule* **2020**, *4* (1), 142−158.

(13) Larsen, T. A.; Riechmann, M. E.; Udert, K. M. State of the Art of Urine Treatment Technologies: A Critical Review. *Water Res.: X* **2021**, *13*, No. 100114.

(14) Sedlak, D.; Mauter, M.; Macknick, J.; Stokes-Draut, J.; Fiske, P.; Agarwal, D.; Borch, T.; Breckenridge, R.; Cath, T.; Chellam, S.; Childress, A.; Dionysiou, D.; Giammar, D.; Hoek, E.; Jiang, S.; Katz, L.; Kim, J.; Kostecki, R.; McCutcheon, J.; Polsky, Y.; Stoll, Z.; Xu, P. *National Alliance for Water Innovation (NAWI) Master Technology Roadmap*; National Renewable Energy Lab (NREL): Golden, CO, 2021.

(15) Chaplin, B. P. The Prospect of Electrochemical Technologies Advancing Worldwide Water Treatment. *Acc. Chem. Res.* **2019**, *52* (3), 596−604.

(16) Radjenovic, J.; Sedlak, D. L. Challenges and Opportunities for Electrochemical Processes as Next-Generation Technologies for the Treatment of Contaminated Water. *Environ. Sci. Technol.* **2015**, *49* (19), 11292−11302.

(17) Kong, L.; Liu, X. Emerging Electrochemical Processes for Materials Recovery from Wastewater: Mechanisms and Prospects. *Front. Environ. Sci. Eng.* **2020**, *14* (5), 90.

(18) Miller, D. M.; Abels, K.; Guo, J.; Williams, K. S.; Liu, M. J.; Tarpeh, W. A. Electrochemical Wastewater Refining: A Vision for Circular Chemical Manufacturing. *J. Am. Chem. Soc.* **2023**, *145*, 19422.

(19) Pronk, W.; Biebow, M.; Boller, M. Electrodialysis for Recovering Salts from a Urine Solution Containing Micropollutants. *Environ. Sci. Technol.* **2006**, *40* (7), 2414−2420.

(20) Desloover, J.; De Vrieze, J.; Van de Vijver, M.; Mortelmans, J.; Rozendal, R.; Rabaey, K. Electrochemical Nutrient Recovery Enables Ammonia Toxicity Control and Biogas Desulfurization in Anaerobic Digestion. *Environ. Sci. Technol.* **2015**, *49* (2), 948−955.

(21) Zhang, C.; Ma, J.; Song, J.; He, C.; Waite, T. D. Continuous Ammonia Recovery from Wastewaters Using an Integrated Capacitive Flow Electrode Membrane Stripping System. *Environ. Sci. Technol.* **2018**, *52* (24), 14275−14285.

(22) Zhang, C.; Ma, J.; Waite, T. D. The Impact of Absorbents on Ammonia Recovery in a Capacitive Membrane Stripping System. *Chem. Eng. J.* **2020**, *382*, No. 122851.

(23) Tarpeh, W. A.; Barazesh, J. M.; Cath, T. Y.; Nelson, K. L. Electrochemical Stripping to Recover Nitrogen from Source-Separated Urine. *Environ. Sci. Technol.* **2018**, *52* (3), 1453−1460.

(24) Li, Y.; Tarpeh, W. A.; Nelson, K. L.; Strathmann, T. J. Quantitative Evaluation of an Integrated System for Valorization of Wastewater Algae as Bio-Oil, Fuel Gas, and Fertilizer Products. *Environ. Sci. Technol.* **2018**, *52* (21), 12717−12727.

(25) Liu, M. J.; Neo, B. S.; Tarpeh, W. A. Building an Operational Framework for Selective Nitrogen Recovery via Electrochemical Stripping. *Water Res.* **2020**, *169*, No. 115226.

(26) Kogler, A.; Farmer, M.; Simon, J. A.; Tilmans, S.; Wells, G. F.; Tarpeh, W. A. Systematic Evaluation of Emerging Wastewater Nutrient Removal and Recovery Technologies to Inform Practice and Advance Resource Efficiency. *ACS EST Eng.* **2021**, *1* (4), 662−684.

(27) Hug, A.; Udert, K. M. Struvite Precipitation from Urine with Electrochemical Magnesium Dosage. *Water Res.* **2013**, *47* (1), 289−299.

(28) Kuntke, P.; Rodríguez Arredondo, M.; Widyakristi, L.; ter Heijne, A.; Sleutels, T. H. J. A.; Hamelers, H. V. M.; Buisman, C. J. N. Hydrogen Gas Recycling for Energy Efficient Ammonia Recovery in Electrochemical Systems. *Environ. Sci. Technol.* **2017**, *51* (5), 3110−3116.

(29) Ward, A. J.; Arola, K.; Thompson Brewster, E.; Mehta, C. M.; Batstone, D. J. Nutrient Recovery from Wastewater through Pilot Scale Electrodialysis. *Water Res.* **2018**, *135*, 57−65.

(30) Fumasoli, A.; Etter, B.; Sterkele, B.; Morgenroth, E.; Udert, K. M. Operating a Pilot-Scale Nitrification/Distillation Plant for Complete Nutrient Recovery from Urine. *Water Sci. Technol.* **2016**, *73* (1), 215−222.

(31) Zamora, P.; Georgieva, T.; Ter Heijne, A.; Sleutels, T. H. J. A.; Jeremiasse, A. W.; Saakes, M.; Buisman, C. J. N.; Kuntke, P. Ammonia Recovery from Urine in a Scaled-up Microbial Electrolysis Cell. *J. Power Sources* **2017**, *356*, 491−499.

(32) Simha, P.; Karlsson, C.; Viskari, E.-L.; Malila, R.; Vinnerås, B. Field Testing a Pilot-Scale System for Alkaline Dehydration of Source-Separated Human Urine: A Case Study in Finland. *Front. Environ. Sci.* **2020**, *8*, No. 570637, DOI: 10.3389/fenvs.2020.570637.
(33) Cid, C. A.; Qu, Y.; Hoffmann, M. R. Design and Preliminary Implementation of Onsite Electrochemical Wastewater Treatment and Recycling Toilets for the Developing World. *Environ. Sci.: Water Res. Technol.* **2018**, *4* (10), 1439−1450.
(34) Mikhaylin, S.; Bazinet, L. Fouling on Ion-Exchange Membranes: Classification, Characterization and Strategies of Prevention and Control. *Adv. Colloid Interface Sci.* **2016**, *229*, 34−56.
(35) Pardo, A.; Otero, E.; Merino, M. C.; López, M. D.; Utrilla, M. V.; Moreno, F. Influence of pH and Chloride Concentration on the Pitting and Crevice Corrosion Behavior of High-Alloy Stainless Steels. *Corrosion* **2000**, *56* (4), 411−418.
(36) Saadawy, M. Kinetics of Pitting Dissolution of Austenitic Stainless Steel 304 in Sodium Chloride Solution. *ISRN Corrosion* **2012**, *2012*, 1−5.
(37) Xu, L. K.; Scantlebury, J. D. A Study on the Deactivation of an IrO2−Ta2O5 Coated Titanium Anode. *Corros. Sci.* **2003**, *45* (12), 2729−2740.
(38) Hu, J. M.; Meng, H. M.; Zhang, J. Q.; Cao, C. N. Degradation Mechanism of Long Service Life Ti/IrO2−Ta2O5 Oxide Anodes in Sulphuric Acid. *Corros. Sci.* **2002**, *44* (8), 1655−1668.
(39) Tarpeh, W. A.; Wald, I.; Omollo, M. O.; Egan, T.; Nelson, K. L. Evaluating Ion Exchange for Nitrogen Recovery from Source-Separated Urine in Nairobi, Kenya. *Dev. Eng.* **2018**, *3*, 188−195.
(40) O'Brien, T.; Bommaraju, T. V.; Hine, F. *Handbook of Chlor-Alkali Technology*; Springer: New York, 2005.
(41) Strathmann, H. Electrodialysis, a Mature Technology with a Multitude of New Applications. *Desalination* **2010**, *264* (3), 268−288.
(42) Goffin, C.; Calay, J. C. Use of Continuous Electrodeionization to Reduce Ammonia Concentration in Steam Generators Blow-down of PWR Nuclear Power Plants. *Desalination* **2000**, *132* (1), 249−253.
(43) Mankins, J. C. *Technology Readiness Levels*; NASA, 1995; p 5.
(44) Institute of Medicine; National Research Council. Technology Readiness Levels in the Department of Defense. In *Technologies to Enable Autonomous Detection for BioWatch: Ensuring Timely and Accurate Information for Public Health Officials: Workshop Summary*; The National Academies Press: Washington, DC, 2014.
(45) Rose, C.; Parker, A.; Jefferson, B.; Cartmell, E. The Characterization of Feces and Urine: A Review of the Literature to Inform Advanced Treatment Technology. *Crit. Rev. Environ. Sci. Technol.* **2015**, *45* (17), 1827−1879.
(46) Larsen, T. A.; Gruendl, H.; Binz, C. The Potential Contribution of Urine Source Separation to the SDG Agenda—a Review of the Progress so Far and Future Development Options. *Environ. Sci.: Water Res. Technol.* **2021**, *7* (7), 1161−1176.
(47) Metrohm Autolab. Basic Overview of the Working Principle of a Potentiostat/Galvanostat (PGSTAT)—Electrochemical Cell Setup (AN-EC-008), 2018. https://www.metrohm.com/en_us/applications/application-notes/autolab-applikationen-anautolab/an-ec-008.html?referrer=https://www.google.com/.
(48) Putnam, D. F. *Composition and Concentrative Properties of Human Urine*; NASA CR-1802; National Aeronautics and Space Administration: Huntington Beach, CA, 1971. https://ntrs.nasa.gov/api/citations/19710023044/downloads/19710023044.pdf.
(49) Park, J.-S.; Choi, J.-H.; Woo, J.-J.; Moon, S.-H. An Electrical Impedance Spectroscopic (EIS) Study on Transport Characteristics of Ion-Exchange Membrane Systems. *J. Colloid Interface Sci.* **2006**, *300* (2), 655−662.
(50) Zhang, W.; Ma, J.; Wang, P.; Wang, Z.; Shi, F.; Liu, H. Investigations on the Interfacial Capacitance and the Diffusion Boundary Layer Thickness of Ion Exchange Membrane Using Electrochemical Impedance Spectroscopy. *J. Membr. Sci.* **2016**, *502*, 37−47.
(51) Gil, V. V.; Andreeva, M. A.; Jansezian, L.; Han, J.; Pismenskaya, N. D.; Nikonenko, V. V.; Larchet, C.; Dammak, L. Impact of Heterogeneous Cation-Exchange Membrane Surface Modification on Chronopotentiometric and Current−Voltage Characteristics in NaCl, CaCl2 and MgCl2 Solutions. *Electrochim. Acta* **2018**, *281*, 472−485.
(52) Barros, K. S.; Martí-Calatayud, M. C.; Pérez-Herranz, V.; Espinosa, D. C. R. A Three-Stage Chemical Cleaning of Ion-Exchange Membranes Used in the Treatment by Electrodialysis of Wastewaters Generated in Brass Electroplating Industries. *Desalination* **2020**, *492*, No. 114628.
(53) McGaughey, A. L.; Gustafson, R. D.; Childress, A. E. Effect of Long-Term Operation on Membrane Surface Characteristics and Performance in Membrane Distillation. *J. Membr. Sci.* **2017**, *543*, 143−150.
(54) Wang, L.; Li, B.; Gao, X.; Wang, Q.; Lu, J.; Wang, Y.; Wang, S. Study of Membrane Fouling in Cross-Flow Vacuum Membrane Distillation. *Sep. Purif. Technol.* **2014**, *122*, 133−143.
(55) Yan, Z.; Yang, H.; Qu, F.; Zhang, H.; Rong, H.; Yu, H.; Liang, H.; Ding, A.; Li, G.; Van der Bruggen, B. Application of Membrane Distillation to Anaerobic Digestion Effluent Treatment: Identifying Culprits of Membrane Fouling and Scaling. *Sci. Total Environ.* **2019**, *688*, 880−889.
(56) Fortunato, L.; Jang, Y.; Lee, J.-G.; Jeong, S.; Lee, S.; Leiknes, T.; Ghaffour, N. Fouling Development in Direct Contact Membrane Distillation: Non-Invasive Monitoring and Destructive Analysis. *Water Res.* **2018**, *132*, 34−41.
(57) Zarebska, A.; Nieto, D. R.; Christensen, K. V.; Norddahl, B. Ammonia Recovery from Agricultural Wastes by Membrane Distillation: Fouling Characterization and Mechanism. *Water Res.* **2014**, *56*, 1−10.
(58) Tijing, L. D.; Woo, Y. C.; Choi, J.-S.; Lee, S.; Kim, S.-H.; Shon, H. K. Fouling and Its Control in Membrane Distillation—A Review. *J. Membr. Sci.* **2015**, *475*, 215−244.
(59) Liao, Y.; Zheng, G.; Huang, J. J.; Tian, M.; Wang, R. Development of Robust and Superhydrophobic Membranes to Mitigate Membrane Scaling and Fouling in Membrane Distillation. *J. Membr. Sci.* **2020**, *601*, No. 117962.
(60) Xiao, Z.; Guo, H.; He, H.; Liu, Y.; Li, X.; Zhang, Y.; Yin, H.; Volkov, A. V.; He, T. Unprecedented Scaling/Fouling Resistance of Omniphobic Polyvinylidene Fluoride Membrane with Silica Nanoparticle Coated Micropillars in Direct Contact Membrane Distillation. *J. Membr. Sci.* **2020**, *599*, No. 117819.
(61) Mondor, M.; Ippersiel, D.; Lamarche, F.; Masse, L. Fouling Characterization of Electrodialysis Membranes Used for the Recovery and Concentration of Ammonia from Swine Manure. *Bioresour. Technol.* **2009**, *100* (2), 566−571.
(62) Kum, S.; Landsman, M. R.; Su, G. M.; Freychet, G.; Lawler, D. F.; Katz, L. E. Performance of a Hybrid ED−NF Membrane System for Water Recovery Improvement via NOM Fouling Control. *ACS EST Eng.* **2021**, *1* (10), 1420−1431.
(63) Ma, G.; Xu, X.; Tesfai, M.; Zhang, Y.; Wang, H.; Xu, P. Nanocomposite Cation-Exchange Membranes for Wastewater Electrodialysis: Organic Fouling, Desalination Performance, and Toxicity Testing. *Sep. Purif. Technol.* **2021**, *275*, No. 119217.
(64) Chen, W.; Qian, C.; Zhou, K.-G.; Yu, H.-Q. Molecular Spectroscopic Characterization of Membrane Fouling: A Critical Review. *Chem* **2018**, *4* (7), 1492−1509.
(65) Soboleva, T.; Xie, Z.; Shi, Z.; Tsang, E.; Navessin, T.; Holdcroft, S. Investigation of the Through-Plane Impedance Technique for Evaluation of Anisotropy of Proton Conducting Polymer Membranes. *J. Electroanal. Chem.* **2008**, *622* (2), 145−152.
(66) Díaz, J. C.; Kamcev, J. Ionic Conductivity of Ion-Exchange Membranes: Measurement Techniques and Salt Concentration Dependence. *J. Membr. Sci.* **2021**, *618*, No. 118718.
(67) Díaz, J. C.; Kitto, D.; Kamcev, J. Accurately Measuring the Ionic Conductivity of Membranes via the Direct Contact Method. *J. Membr. Sci.* **2023**, *669*, No. 121304.
(68) Ohki, T.; Nishikawa, N.; Hasegawa, T.; Okano, T.; Tanizawa, Y. Characterization of Scale Formed on the Surfaces of Toilet Bowls. *J. Surfactants Deterg.* **2010**, *13* (1), 19−26.

(69) Udert, K. M.; Larsen, T. A.; Biebow, M.; Gujer, W. Urea Hydrolysis and Precipitation Dynamics in a Urine-Collecting System. *Water Res.* **2003**, *37* (11), 2571−2582.
(70) Rodríguez Arredondo, M.; Kuntke, P.; ter Heijne, A.; Hamelers, H. V. M.; Buisman, C. J. N. Load Ratio Determines the Ammonia Recovery and Energy Input of an Electrochemical System. *Water Res.* **2017**, *111*, 330−337.
(71) Kuntke, P.; Rodrigues, M.; Sleutels, T.; Saakes, M.; Hamelers, H. V. M.; Buisman, C. J. N. Energy-Efficient Ammonia Recovery in an Up-Scaled Hydrogen Gas Recycling Electrochemical System. *ACS Sustainable Chem. Eng.* **2018**, *6* (6), 7638−7644.
(72) Wilsenach, J.; Van Loosdrecht, M. Impact of Separate Urine Collection on Wastewater Treatment Systems. *Water Sci. Technol.* **2003**, *48* (1), 103−110.
(73) Jimenez, J.; Bott, C.; Love, N.; Bratby, J. Source Separation of Urine as an Alternative Solution to Nutrient Management in Biological Nutrient Removal Treatment Plants. *Water Environ. Res.* **2015**, *87* (12), 2120−2129.
(74) Landry, K. A.; Boyer, T. H. Life Cycle Assessment and Costing of Urine Source Separation: Focus on Nonsteroidal Anti-Inflammatory Drug Removal. *Water Res.* **2016**, *105*, 487−495.
(75) Ishii, S. K. L.; Boyer, T. H. Life Cycle Comparison of Centralized Wastewater Treatment and Urine Source Separation with Struvite Precipitation: Focus on Urine Nutrient Management. *Water Res.* **2015**, *79*, 88−103.
(76) Gunnarsson, M.; Lalander, C.; McConville, J. R. Estimating Environmental and Societal Impacts from Scaling up Urine Concentration Technologies. *J. Cleaner Prod.* **2023**, *382*, No. 135194.
(77) Rodrigues, M.; Lund, R. J.; ter Heijne, A.; Sleutels, T.; Buisman, C. J. N.; Kuntke, P. Application of Ammonium Fertilizers Recovered by an Electrochemical System. *Resour., Conserv. Recycl.* **2022**, *181*, No. 106225.
(78) The Seven Most Common Grades for Chemicals and Reagents. Lab Manager, 2023. https://www.labmanager.com/the-seven-most-common-grades-for-chemicals-and-reagents-2655.
(79) Xu, X.; Du, X.; Wang, F.; Sha, J.; Chen, Q.; Tian, G.; Zhu, Z.; Ge, S.; Jiang, Y. Effects of Potassium Levels on Plant Growth, Accumulation and Distribution of Carbon, and Nitrate Metabolism in Apple Dwarf Rootstock Seedlings. *Front. Plant Sci.* **2020**, *11*, No. 904, DOI: 10.3389/fpls.2020.00904.
(80) Butcher, K.; Wick, A. F.; DeSutter, T.; Chatterjee, A.; Harmon, J. Soil Salinity: A Threat to Global Food Security. *Agron. J.* **2016**, *108* (6), 2189−2200.
(81) Fumasep FKS-50, 2023. https://www.fuelcellstore.com/fumasep-fks.
(82) Pall Corporation. *Product Safety Data Information: Versapor® RC Membranes*; Pall Corporation, 2019.
(83) Fan, H.; Huang, Y.; Yip, N. Y. Advancing Ion-Exchange Membranes to Ion-Selective Membranes: Principles, Status, and Opportunities. *Front. Environ. Sci. Eng.* **2023**, *17* (2), 25.
(84) Krödel, M.; Carter, B. M.; Rall, D.; Lohaus, J.; Wessling, M.; Miller, D. J. Rational Design of Ion Exchange Membrane Material Properties Limits the Crossover of CO2 Reduction Products in Artificial Photosynthesis Devices. *ACS Appl. Mater. Interfaces* **2020**, *12* (10), 12030−12042.
(85) Roman, M.; Van Dijk, L. H.; Gutierrez, L.; Vanoppen, M.; Post, J. W.; Wols, B. A.; Cornelissen, E. R.; Verliefde, A. R. D. Key Physicochemical Characteristics Governing Organic Micropollutant Adsorption and Transport in Ion-Exchange Membranes during Reverse Electrodialysis. *Desalination* **2019**, *468*, No. 114084.
(86) The Engineering ToolBox. Solubility of Gases in Water vs. Temperature, 2023. https://www.engineeringtoolbox.com/gases-solubility-water-d_1148.html.
(87) Lucile, F.; Cézac, P.; Contamine, F.; Serin, J.-P.; Houssin, D.; Arpentinier, P. Solubility of Carbon Dioxide in Water and Aqueous Solution Containing Sodium Hydroxide at Temperatures from (293.15 to 393.15) K and Pressure up to 5 MPa: Experimental Measurements. *J. Chem. Eng. Data* **2012**, *57* (3), 784−789.
(88) Rumpf, B.; Xia, J.; Maurer, G. Solubility of Carbon Dioxide in Aqueous Solutions Containing Acetic Acid or Sodium Hydroxide in the Temperature Range from 313 to 433 K and at Total Pressures up to 10 MPa. *Ind. Eng. Chem. Res.* **1998**, *37* (5), 2012−2019.
(89) Schreiber, T.; Opperman, S.; Hardin, R.; Cavicchi, J.; Pallmeyer, A.; Nace, K.; Love, N. Nested Risks and Responsibilities: Perspectives on Fertilizer from Human Urine in Two U.S. Regions. *J. Agric. Food Syst. Community Dev.* **2021**, *10* (3), 221−242.
(90) Rouwenhorst, K. H. R.; Krzywda, P. M.; Benes, N. E.; Mul, G.; Lefferts, L. Ammonia Production Technologies. In *Techno-Economic Challenges of Green Ammonia as an Energy Vector*; Valera-Medina, A., Banares-Alcantara, R., Eds.; Academic Press, 2021; Chapter 4, pp 41−83. DOI: 10.1016/B978-0-12-820560-0.00004-7.
(91) Maurer, M.; Schwegler, P.; Larsen, T. A. Nutrients in Urine: Energetic Aspects of Removal and Recovery. *Water Sci. Technol.* **2003**, *48* (1), 37−46.
(92) Strathmann, H.; Grabowski, A.; Eigenberger, G. Ion-Exchange Membranes in the Chemical Process Industry. *Ind. Eng. Chem. Res.* **2013**, *52* (31), 10364−10379.
(93) Barros, K. S.; Martí-Calatayud, M. C.; Scarazzato, T.; Bernardes, A. M.; Espinosa, D. C. R.; Pérez-Herranz, V. Investigation of Ion-Exchange Membranes by Means of Chronopotentiometry: A Comprehensive Review on This Highly Informative and Multipurpose Technique. *Adv. Colloid Interface Sci.* **2021**, *293*, No. 102439.
(94) Andreeva, M. A.; Gil, V. V.; Pismenskaya, N. D.; Dammak, L.; Kononenko, N. A.; Larchet, C.; Grande, D.; Nikonenko, V. V. Mitigation of Membrane Scaling in Electrodialysis by Electroconvection Enhancement, pH Adjustment and Pulsed Electric Field Application. *J. Membr. Sci.* **2018**, *549*, 129−140.
(95) Chilcott, T. C.; Chan, M.; Gaedt, L.; Nantawisarakul, T.; Fane, A. G.; Coster, H. G. L. Electrical Impedance Spectroscopy Characterisation of Conducting Membranes: I. Theory. *J. Membr. Sci.* **2002**, *195* (2), 153−167.
(96) Gaedt, L.; Chilcott, T. C.; Chan, M.; Nantawisarakul, T.; Fane, A. G.; Coster, H. G. L. Electrical Impedance Spectroscopy Characterisation of Conducting Membranes: II. Experimental. *J. Membr. Sci.* **2002**, *195* (2), 169−180.
(97) Mareev, S. A.; Nebavskiy, A. V.; Nichka, V. S.; Urtenov, M. K.; Nikonenko, V. V. The Nature of Two Transition Times on Chronopotentiograms of Heterogeneous Ion Exchange Membranes: 2D Modelling. *J. Membr. Sci.* **2019**, *575*, 179−190.
(98) Butylskii, D. Y.; Mareev, S. A.; Pismenskaya, N. D.; Apel, P. Y.; Polezhaeva, O. A.; Nikonenko, V. V. Phenomenon of Two Transition Times in Chronopotentiometry of Electrically Inhomogeneous Ion Exchange Membranes. *Electrochim. Acta* **2018**, *273*, 289−299.
(99) Guillen-Burrieza, E.; Ruiz-Aguirre, A.; Zaragoza, G.; Arafat, H. A. Membrane Fouling and Cleaning in Long Term Plant-Scale Membrane Distillation Operations. *J. Membr. Sci.* **2014**, *468*, 360−372.
(100) Lin, S.; Nejati, S.; Boo, C.; Hu, Y.; Osuji, C. O.; Elimelech, M. Omniphobic Membrane for Robust Membrane Distillation. *Environ. Sci. Technol. Lett.* **2014**, *1* (11), 443−447.
(101) Bauer, A.; Wagner, M.; Saravia, F.; Bartl, S.; Hilgenfeldt, V.; Horn, H. In-Situ Monitoring and Quantification of Fouling Development in Membrane Distillation by Means of Optical Coherence Tomography. *J. Membr. Sci.* **2019**, *577*, 145−152.
(102) Dow, N.; Gray, S.; Li, J.; Zhang, J.; Ostarcevic, E.; Liubinas, A.; Atherton, P.; Roeszler, G.; Gibbs, A.; Duke, M. Pilot Trial of Membrane Distillation Driven by Low Grade Waste Heat: Membrane Fouling and Energy Assessment. *Desalination* **2016**, *391*, 30−42.
(103) Horseman, T.; Yin, Y.; Christie, K. S.; Wang, Z.; Tong, T.; Lin, S. Wetting, Scaling, and Fouling in Membrane Distillation: State-of-the-Art Insights on Fundamental Mechanisms and Mitigation Strategies. *ACS EST Eng.* **2021**, *1* (1), 117−140.
(104) Zhong, C.; Deng, Y.; Hu, W.; Qiao, J.; Zhang, L.; Zhang, J. A Review of Electrolyte Materials and Compositions for Electrochemical Supercapacitors. *Chem. Soc. Rev.* **2015**, *44* (21), 7484−7539.
(105) Al-Amshawee, S.; Yunus, M. Y. B. M.; Azoddein, A. A. M.; Hassell, D. G.; Dakhil, I. H.; Hasan, H. A. Electrodialysis Desalination

for Water and Wastewater: A Review. *Chem. Eng. J.* **2020**, *380*, No. 122231.
(106) Gally, C. R.; Benvenuti, T.; da Trindade, C. d. M.; Rodrigues, M. A. S.; Zoppas-Ferreira, J.; Pérez-Herranz, V.; Bernardes, A. M. Electrodialysis for the Tertiary Treatment of Municipal Wastewater: Efficiency of Ion Removal and Ageing of Ion Exchange Membranes. *J. Environ. Chem. Eng.* **2018**, *6* (5), 5855−5869.
(107) Ghalloussi, R.; Garcia-Vasquez, W.; Chaabane, L.; Dammak, L.; Larchet, C.; Deabate, S. V.; Nevakshenova, E.; Nikonenko, V.; Grande, D. Ageing of Ion-Exchange Membranes in Electrodialysis: A Structural and Physicochemical Investigation. *J. Membr. Sci.* **2013**, *436*, 68−78.
(108) Bdiri, M.; Dammak, L.; Chaabane, L.; Larchet, C.; Hellal, F.; Nikonenko, V.; Pismenskaya, N. D. Cleaning of Cation-Exchange Membranes Used in Electrodialysis for Food Industry by Chemical Solutions. *Sep. Purif. Technol.* **2018**, *199*, 114−123.
(109) Yeo, R. S.; McBreen, J.; Kissel, G.; Kulesa, F.; Srinivasan, S. Perfluorosulphonic Acid (Nafion) Membrane as a Separator for an Advanced Alkaline Water Electrolyser. *J. Appl. Electrochem.* **1980**, *10* (6), 741−747.
(110) Solvay. Aquivion® Powder PW79S. Solvay, 2023. https://www.solvay.com/en/product/aquivion-powder-pw79s.
(111) Chen, W.; Zhang, M.-K.; Liu, B.-Y.; Cai, J.; Chen, Y.-X. Challenges and Recent Progress in Unraveling the Intrinsic pH Effect in Electrocatalysis. *Curr. Opin. Electrochem.* **2022**, *34*, No. 101003.
(112) Fornaciari, J. C.; Weng, L.-C.; Alia, S. M.; Zhan, C.; Pham, T. A.; Bell, A. T.; Ogitsu, T.; Danilovic, N.; Weber, A. Z. Mechanistic Understanding of pH Effects on the Oxygen Evolution Reaction. *Electrochim. Acta* **2022**, *405*, No. 139810.
(113) Auinger, M.; Katsounaros, I.; Meier, J. C.; Klemm, S. O.; Biedermann, P. U.; Topalov, A. A.; Rohwerder, M.; Mayrhofer, K. J. J. Near-Surface Ion Distribution and Buffer Effects during Electrochemical Reactions. *Phys. Chem. Chem. Phys.* **2011**, *13* (36), 16384.
(114) Katsounaros, I.; Meier, J. C.; Klemm, S. O.; Topalov, A. A.; Biedermann, P. U.; Auinger, M.; Mayrhofer, K. J. J. The Effective Surface pH during Reactions at the Solid−Liquid Interface. *Electrochem. Commun.* **2011**, *13* (6), 634−637.
(115) Garcia-Vasquez, W.; Ghalloussi, R.; Dammak, L.; Larchet, C.; Nikonenko, V.; Grande, D. Structure and Properties of Heterogeneous and Homogeneous Ion-Exchange Membranes Subjected to Ageing in Sodium Hypochlorite. *J. Membr. Sci.* **2014**, *452*, 104−116.
(116) Thakur, A. K.; Malmali, M. Advances in Polymeric Cation Exchange Membranes for Electrodialysis: An Overview. *J. Environ. Chem. Eng.* **2022**, *10* (5), No. 108295.
(117) Choudhury, M. R.; Anwar, N.; Jassby, D.; Rahaman, M. S. Fouling and Wetting in the Membrane Distillation Driven Wastewater Reclamation Process—A Review. *Adv. Colloid Interface Sci.* **2019**, *269*, 370−399.
(118) Alkhatib, A.; Ayari, M. A.; Hawari, A. H. Fouling Mitigation Strategies for Different Foulants in Membrane Distillation. *Chem. Eng. Process.* **2021**, *167*, No. 108517.
(119) Abdel-Karim, A.; Leaper, S.; Skuse, C.; Zaragoza, G.; Gryta, M.; Gorgojo, P. Membrane Cleaning and Pretreatments in Membrane Distillation—a Review. *Chem. Eng. J.* **2021**, *422*, No. 129696.
(120) Hsieh, I.-M.; Thakur, A. K.; Malmali, M. Comparative Analysis of Various Pretreatments to Mitigate Fouling and Scaling in Membrane Distillation. *Desalination* **2021**, *509*, No. 115046.
(121) Warsinger, D. M.; Swaminathan, J.; Guillen-Burrieza, E.; Arafat, H. A.; Lienhard V, J. H. Scaling and Fouling in Membrane Distillation for Desalination Applications: A Review. *Desalination* **2015**, *356*, 294−313.
(122) Merino-Garcia, I.; Velizarov, S. New Insights into the Definition of Membrane Cleaning Strategies to Diminish the Fouling Impact in Ion Exchange Membrane Separation Processes. *Sep. Purif. Technol.* **2021**, *277*, No. 119445.
(123) Zhou, W.; Chen, Y.; He, X.; Wang, Z. Mechanistic Insights to the Reversibility of Membrane Wetting in Membrane Distillation. *J. Membr. Sci.* **2023**, *685*, No. 121958.
(124) Yang, K.; Qin, M. The Application of Cation Exchange Membranes in Electrochemical Systems for Ammonia Recovery from Wastewater. *Membranes* **2021**, *11* (7), 494.
(125) Liu, H.; She, Q. Influence of Membrane Structure-Dependent Water Transport on Conductivity-Permselectivity Trade-off and Salt/Water Selectivity in Electrodialysis: Implications for Osmotic Electrodialysis Using Porous Ion Exchange Membranes. *J. Membr. Sci.* **2022**, *650*, No. 120398.
(126) Ray, H.; Saetta, D.; H. Boyer, T. Characterization of Urea Hydrolysis in Fresh Human Urine and Inhibition by Chemical Addition. *Environ. Sci.: Water Res. Technol.* **2018**, *4* (1), 87−98.
(127) Randall, D. G.; Krähenbühl, M.; Köpping, I.; Larsen, T. A.; Udert, K. M. A Novel Approach for Stabilizing Fresh Urine by Calcium Hydroxide Addition. *Water Res.* **2016**, *95*, 361−369.
(128) Reddy, K. R. C.; Kayastha, A. M. Improved Stability of Urease upon Coupling to Alkylamine and Arylamine Glass and Its Analytical Use. *J. Mol. Catal. B: Enzym.* **2006**, *38* (2), 104−112.
(129) Blakeley, R. L.; Treston, A.; Andrews, R. K.; Zerner, B. Nickel(II)-Promoted Ethanolysis and Hydrolysis of N-(2-Pyridylmethyl)Urea. A Model for Urease. *J. Am. Chem. Soc.* **1982**, *104* (2), 612−614.
(130) Simka, W.; Piotrowski, J.; Nawrat, G. Influence of Anode Material on Electrochemical Decomposition of Urea. *Electrochim. Acta* **2007**, *52* (18), 5696−5703.
(131) Cataldo Hernández, M.; Russo, N.; Panizza, M.; Spinelli, P.; Fino, D. Electrochemical Oxidation of Urea in Aqueous Solutions Using a Boron-Doped Thin-Film Diamond Electrode. *Diamond Relat. Mater.* **2014**, *44*, 109−116.
(132) Schranck, A.; Doudrick, K. Effect of Reactor Configuration on the Kinetics and Nitrogen Byproduct Selectivity of Urea Electrolysis Using a Boron Doped Diamond Electrode. *Water Res.* **2020**, *168*, No. 115130.
(133) Vedharathinam, V.; Botte, G. G. Understanding the Electro-Catalytic Oxidation Mechanism of Urea on Nickel Electrodes in Alkaline Medium. *Electrochim. Acta* **2012**, *81*, 292−300.
(134) ChemAnalyst. Ammonium Sulphate Price Trend and Forecast, 2023. https://www.chemanalyst.com/Pricing-data/ammonium-sulphate-64.
(135) Yang, Z.; Du, X.; Lu, L.; Tejeda, H. Price and Volatility Transmissions among Natural Gas, Fertilizer, and Corn Markets: A Revisit. *J. Risk Financ. Manag.* **2022**, *15* (2), 91.
(136) Nti, F. K. International Agricultural Trade Report. In *Impacts and Repercussions of Price Increases on the Global Fertilizer Market*; U.S. Department of Agriculture Foreign Agricultural Service, 2022. https://www.fas.usda.gov/data/impacts-and-repercussions-price-increases-global-fertilizer-market.
(137) Baffes, J.; Wee Chian, K. Fertilizer Prices Expected to Remain Higher for Longer. World Bank Blogs, 2023. https://blogs.worldbank.org/opendata/fertilizer-prices-expected-remain-higher-longer.
(138) Food and Agriculture Organization of the United Nations; World Trade Organization. Global Fertilizer Markets and Policies: A Joint FAO/WTO Mapping Exercise, 2022. https://www.wto.org/english/news_e/news22_e/igo_14nov22_epdf.
(139) US Department of Agriculture Economic Research Service. Table 7. Average U.S. Farm Prices of Selected Fertilizers, 2019. https://www.ers.usda.gov/data-products/fertilizer-use-and-price/.
(140) U.S. Bureau of Labor Statistics. Consumer Price Index for All Urban Consumers: All Items in U.S. City Average, 2023. https://fred.stlouisfed.org/series/CPIAUCSL.
(141) U.S. Bureau of Labor Statistics. PPI Industry Data for Nitrogenous Fertilizer Manufacturing-Synthetic Ammonia, Nitric Acid, Ammonium Compounds, and Urea, Not Seasonally Adjusted, 2023. https://beta.bls.gov/dataViewer/view/timeseries/PCU325311132531 1A;jsessionid=E2CCD7F442F55D939A894D90DAF9988D.
(142) Comer, B. M.; Fuentes, P.; Dimkpa, C. O.; Liu, Y.-H.; Fernandez, C. A.; Arora, P.; Realff, M.; Singh, U.; Hatzell, M. C.; Medford, A. J. Prospects and Challenges for Solar Fertilizers. *Joule* **2019**, *3* (7), 1578−1605.

(143) McArthur, J. W.; McCord, G. C. Fertilizing Growth: Agricultural Inputs and Their Effects in Economic Development. *J. Dev. Econ.* **2017**, *127*, 133−152.
(144) Huang, X.; Guida, S.; Jefferson, B.; Soares, A. Economic Evaluation of Ion-Exchange Processes for Nutrient Removal and Recovery from Municipal Wastewater. *npj Clean Water* **2020**, 3 (1), 7.
(145) Pan, S.; Li, H.; Liu, D.; Huang, R.; Pan, X.; Ren, D.; Li, J.; Shakouri, M.; Zhang, Q.; Wang, M.; Wei, C.; Mai, L.; Zhang, B.; Zhao, Y.; Wang, Z.; Graetzel, M.; Zhang, X. Efficient and Stable Noble-Metal-Free Catalyst for Acidic Water Oxidation. *Nat. Commun.* **2022**, *13* (1), No. 2294.
(146) Li, A.; Kong, S.; Guo, C.; Ooka, H.; Adachi, K.; Hashizume, D.; Jiang, Q.; Han, H.; Xiao, J.; Nakamura, R. Enhancing the Stability of Cobalt Spinel Oxide towards Sustainable Oxygen Evolution in Acid. *Nat. Catal.* **2022**, *5* (2), 109−118.
(147) Zhao, L.; Cao, Q.; Wang, A.; Duan, J.; Zhou, W.; Sang, Y.; Liu, H. Iron Oxide Embedded Titania Nanowires—An Active and Stable Electrocatalyst for Oxygen Evolution in Acidic Media. *Nano Energy* **2018**, *45*, 118−126.
(148) Hasseler, T. D.; Ramachandran, A.; Tarpeh, W. A.; Stadermann, M.; Santiago, J. G. Process Design Tools and Techno-Economic Analysis for Capacitive Deionization. *Water Res.* **2020**, *183*, No. 116034.
(149) Parker, D. S. Introduction of New Process Technology into the Wastewater Treatment Sector. *Water Environ. Res.* **2011**, *83* (6), 483−497.

https://doi.org/10.1021/acsenvironau.3c00058
ACS Environ. Au 2024, 4, 89−105